

Early Dark Energy from a Higher-dimensional Gauge Theory

Kentaro Kojima^{a,1} and Yuri Okubo^{b,2}

^a *Faculty of Arts and Science, Kyushu University, Fukuoka 819-0395, Japan*

^b *Graduate School of Science, Kyushu University, Fukuoka 819-0395, Japan*

Abstract

The Hubble constant estimated from the CMB measurements shows large disagreement with the locally measured value. This inconsistency is called the Hubble tension and is vastly studied in recent years. Early Dark Energy (EDE) gives a few percent contribution to the total energy density of the universe only at an epoch before the recombination, and it is considered as a promising solution to the tension. A simple realization of EDE is given by dynamics of a scalar field, called the EDE scalar, and models including the EDE scalar are extensively studied in the literature. In this paper, we present a novel EDE scenario based on higher-dimensional gauge theories. An extra component of gauge fields associated with a compact extra dimension behaves as the EDE scalar at low-energy and has a periodic potential, which has a similar form as potentials for pseudo Nambu-Goldstone bosons (PNGB). In a five-dimensional $U(1)$ gauge theory, we show that a scalar field that originates from the gauge field can give EDE through its dynamics in a PNGB type potential with a suitable choice of parameters in the theory. We focus on the scenario where EDE is explained by the scalar field and clarify constraints on the fundamental parameters of the gauge theory, such as the gauge coupling, the compactification scale, and the mass parameters for matter fields. We also find that a sufficient dilution of EDE requires non-trivial relations among $U(1)$ charges of matter fields with degenerate bulk masses. The required bulk matter contents and $U(1)$ charges can be given by hand and may be realized more naturally through underlying mechanisms such as flavor symmetries. With specific matter contents, we numerically solve the time evolution of the scalar field and confirm that its energy density behaves as an EDE. In our scenario, the parameters of the gauge theory and predicted properties of EDE are related to each other. Thus, the cosmological restrictions on the EDE properties provide insights into higher-dimensional gauge theories.

¹E-mail: kojima@artsci.kyushu-u.ac.jp

²E-mail: okubo.yuri@phys.kyushu-u.ac.jp

1 Introduction

The expansion rate of the present universe is described by the Hubble constant H_0 , whose value is determined through observations. Precise observations and studies of the cosmic microwave background (CMB) determine the Hubble constant as $H_0 = 67.4 \pm 0.5 \text{ km s}^{-1} \text{ Mpc}^{-1}$ by assuming the Λ CDM model of the universe [1]. Independently of the CMB measurements, the Hubble constant is also determined through the cosmic distance ladder. Recent observations of Cepheid variable stars and Type Ia supernovae as distance indicators by the SH0ES project determine the local value of the Hubble constant as $H_0 = 74.03 \pm 1.42 \text{ km s}^{-1} \text{ Mpc}^{-1}$ [2]. There is a large discrepancy, called the Hubble tension, in the H_0 values inferred from CMB observations and obtained from the local measurements. The recent analysis shows a 5σ difference between them [3]. Since the Hubble tension arises under the assumption of the Λ CDM model, this tension may be resolved by new physics beyond the Λ CDM cosmology.

Motivated by the Hubble tension, extensions of the standard cosmology have been widely discussed in recent years [4]. For example, models with extra radiation have been studied [5–10]. In these scenarios, additional relativistic degrees of freedom to the Standard Model (SM) of elementary particles increase the value of the Hubble constant inferred from CMB measurements. The Hubble tension has also been studied in models assuming extra interactions [11, 12], critical phenomena [13], and modified gravity [14–18]. In addition, modifications of dark energy properties at late times have been studied. For instance, the Hubble tension can be resolved by introducing phantom dark energy, whose value of the equation of state (EoS) deviates from the Λ CDM value $w = -1$ and satisfies $w < -1$ [19, 20]. There also exist other late-time modifications of dark energy properties [21–27] and various theoretical approaches focusing on the discrepancy of the Hubble constant.

On the other hand, early-time modifications of the universe from the Λ CDM model have been widely discussed, motivated by the Hubble tension. Among them, the idea of early dark energy (EDE) is one of the promising scenarios [28–31]. In EDE models, the cosmic expansion is slightly modified from the Λ CDM case since an additional source of dark energy, called EDE, gives a few percent contribution to the total energy of the universe before the recombination. Then, the EDE density decreases faster than the matter energy density and becomes negligible, as required not to affect the cosmic expansion after the recombination. While the EDE scenario is restricted through the other observable quantities other than H_0 [32], the additional energy offered by EDE increases the inferred value of H_0 from the CMB data and is favored for solving the Hubble tension. Recently, many models and analyses related to EDE have been studied [33–44].

The EoS of EDE must depend on time. A simple realization of the time dependence is given by the time evolution of scalar fields, as in various models of the inflation [45] and quintessence [46]. In general, kinetic and potential energies of scalar fields contribute to the energy density of the universe. Let w_ϕ be the value of the EoS of EDE that is supposed to be determined by a scalar field ϕ , referred to as the EDE scalar. For a stationary configuration of the EDE scalar, $w_\phi \simeq -1$ is obtained. On the other hand, if the EDE scalar moves rapidly in its potential, then w_ϕ increases and deviates from -1 . Thus, by using the time evolution, scalar fields can explain the time dependence of the EoS.

Several models describing the EDE scalar have been recently proposed. The observed scalar fields, which are fundamentally described by SM of elementary particles, cannot be identified as the EDE scalar. Thus, if the dynamics of scalar fields give the EDE, extensions of the SM are not evaded. Therefore, the Hubble tension may also be a key to physics beyond the SM. A variety of models that incorporate physics beyond the SM is studied to describe the EDE scalar. For example, an axion-dilaton coupled system is studied [36], where dilaton rolls down a runaway type potential and gives energy density contributions that have EDE-like behavior. Also, a power-law type potential for the EDE scalar ϕ , *i.e.*, $V(\phi) \propto \phi^{2n}$, is valid to solve the Hubble tension as discussed in the literature [35, 41]. If a scalar field ϕ oscillates in the power-law potential, the time-averaged EoS $\langle w_\phi \rangle$, related to the scalar energy density, is given by $\langle w_\phi \rangle \simeq (n-1)/(n+1)$ [47]. Thus, for $n \geq 2$, the EDE density decreases faster than the matter energy density as required. In ref. [41], by using *Planck* 2018+SPTPol (TT & EE)+SPTLensing+ S_8 prior datasets, the Hubble constant inferred by CMB data is shown to be increased as $H_0 = 73.06 \pm 1.26 \text{ km s}^{-1} \text{ Mpc}^{-1}$ for $n = 3$.

This paper focuses on the EDE scenario where the EDE scalar evolves in a periodic potential, which is a typical one for pseudo Nambu-Goldstone bosons (PNGBs). Such periodic potentials, which we call PNGB type potentials, have been investigated and considered promising to explain EDE [30, 31]. We discuss the EDE scalar ϕ with the PNGB potential $V(\phi) \propto (1 - \cos[\phi/f])^n$, where f is a mass parameter and n is an integer. In models with axion-like particles, which are a familiar realization of PNGB, potentials are often considered to be generated through non-perturbative effects. In these cases, we naturally expect that $n = 1$ contributions exist in PNGB type potentials unless there is some unknown mechanism or fine-tuning. On the other hand, the $n = 1$ contribution is implied to vanish if EDE provides a resolution to the Hubble tension [34]. Thus, it is expected to reveal the origin of the EDE scalar with the $n \geq 2$ PNGB type potential.

In this paper, we explore the validity of five-dimensional (5D) $U(1)$ gauge theories with a compact space as a specific origin of the EDE scalar. Higher-dimensional gauge theories are predicted in string theories and are motivated candidates for physics beyond the SM. In 5D gauge theories, a four-dimensional (4D) scalar field appears at low energy, which originates from the extra component of the gauge field A_5 . Previous studies have shown that A_5 is a good candidate for an inflaton field [48] or a quintessence field [49]. As shown below, A_5 is also a suitable candidate for the EDE scalar. One advantage of this scenario is the consequence of a particular property of the potential for A_5 . Due to the gauge symmetry, the potential is completely flat at the classical level and is radiatively induced. The potential form is highly restricted since the physical degrees of freedom are not carried by A_5 but by a Wilson line phase, which is a gauge-invariant and non-local quantity. The resultant potential has a periodicity, as seen in the PNGB potential, and we obtain the EDE scalar with a PNGB potential in 5D gauge theories. Moreover, we find that the PNGB potential with $n \geq 2$, required to resolve the Hubble tension, is derived by using perturbative calculations in some concrete models. In our scenario, as a result, the fundamental parameters in 5D gauge theories, such as the gauge coupling constant and the compactification scale, control the potential for the EDE scalar and are related to EDE properties.

This paper is organized as follows. In Sec. 2, we review and study the EDE scenario

provided by the EDE scalar with the PANGB type potential. We discuss constraints on parameters of the potential to obtain adequate EDE for resolving or relaxing the Hubble tension. In Sec. 3, we introduce 5D $U(1)$ gauge theories as a specific origin of the EDE scalar. Based on the one-loop effective potential for the EDE scalar, we study constraints on the mass scales appearing in 5D gauge theories. In Sec. 4, we continue to discuss the 5D gauge theories assuming concrete bulk matter contents as examples. In this case, the EDE scalar potential depends only on a few parameters. We also give numerical studies of the time evolution of the EDE scalar and its energy density parameter. Sec. 5 is devoted to discussions and conclusions. We derive a formula used in our discussion in the appendix.

2 Constraints on the PANGB potential for the EDE scalar field

This section reviews the EDE resolution to the Hubble tension implemented by dynamics of scalar fields. We mainly discuss the case that the EDE scalar has a PANGB type potential. As seen below, the potential parameters are constrained to give suitable contributions to the total energy density of the universe to resolve the Hubble tension.

In the following, we assume the homogeneous, isotropic, and flat spacetime, described by the Friedmann-Lemaître-Robertson-Walker (FLRW) metric, as an approximation of the universe. The cosmic expansion is parametrized by the scale factor $a(t)$, which is the function of time t . We also use the redshift $z(t) = a(t_0)/a(t) - 1$, where t_0 is the present time. The Hubble parameter is given by $H(t) = \dot{a}(t)/a(t)$, where the dot denotes the time derivative. The Hubble constant H_0 is the present value of the Hubble parameter, *i.e.*, $H_0 = H(t_0)$.

The Hubble parameter $H(t)$ describes the expansion rate of the universe and is determined by the energy density of the universe $\rho(z)$, which we define as the function of the redshift. In the Λ CDM model, $\rho(z)$ consists of contributions from the non-relativistic matter $\rho_m(z)$, radiation $\rho_r(z)$, and cosmological constant $\rho_{\Lambda,0}$. In addition to these Λ CDM contributions, we suppose that $\rho(z)$ contains a non-negligible contribution $\rho_\phi(z)$, related to the EDE scalar. Thus, the total energy density is written as

$$\rho(z) = \rho_m(z) + \rho_r(z) + \rho_{\Lambda,0} + \rho_\phi(z). \quad (2.1)$$

We hereafter use $\rho_{m,0} \equiv \rho_m(0)$ and $\rho_{r,0} \equiv \rho_r(0)$.

The time evolution of the scale factor is determined by the following Friedmann equation:

$$3M_{\text{P}}^2 H^2 = \rho(z) = \rho_{m,0}(1+z)^3 + \rho_{r,0}(1+z)^4 + \rho_{\Lambda,0} + \rho_\phi(z), \quad (2.2)$$

where $M_{\text{P}} = (8\pi G)^{-1/2} \simeq 2.4 \times 10^{18}$ GeV is the reduced Planck mass, and G is the gravitational constant. In the Λ CDM model, we can rewrite Eq. (2.2) as

$$H = \bar{H}_0 \sqrt{\Omega_{m,0} h^2 (1+z)^3 + \Omega_{r,0} h^2 (1+z)^4 + \Omega_{\Lambda,0} h^2}, \quad (2.3)$$

where $\Omega_{x,0} \equiv \rho_{x,0}/\rho(0)$ ($x = m, r, \Lambda$) are the energy density parameters, and h is H_0 in units of $\bar{H}_0 = 100 \text{ km s}^{-1} \text{ Mpc}^{-1}$. By definition, the density parameters satisfy

$$\Omega_{m,0} + \Omega_{r,0} + \Omega_{\Lambda,0} = 1, \quad 0 \leq \Omega_{x,0} \leq 1, \quad (x = m, r, \Lambda). \quad (2.4)$$

Thus, the parameters $\Omega_{x,0}$ and h determine the time evolution of $H(z)$ in the Λ CDM model.

The cosmological parameters can be determined by CMB observations. While the curvature is also determined by the observations, we ignore it for simplicity. The energy density parameter of the photon $\Omega_{\gamma,0}$ can be obtained from the CMB averaged temperature T_0 as $\Omega_{\gamma,0}h^2 = 2.47 \times 10^{-5}$ for $T_0 = 2.725 \text{ K}$ [50]. We can include the neutrino contribution by using the relation $\Omega_{r,0} = (1 + 0.227N_{\text{eff}})\Omega_{\gamma,0}$, where N_{eff} is the relativistic degrees of freedom of neutrinos [51], and we get $\Omega_{r,0}h^2 = 4.18 \times 10^{-5}$ from the SM prediction $N_{\text{eff}} = 3.044$ [52]. The CMB power spectrum determines values of $\Omega_{m,0}$ and the baryon matter density parameter $\Omega_{b,0}$. The ratio of even-numbered to odd-numbered peak amplitudes depends on $\Omega_{b,0}h^2$, and the ratio of the first peak to the other peaks depends on $\Omega_{m,0}h^2$. For example, *Planck* project gives $\Omega_{b,0}h^2 = 0.0224 \pm 0.0001$ and $\Omega_{m,0}h^2 = 0.143 \pm 0.001$ [1]. From these results, the energy densities of matter and radiation coincident at $z_{\text{eq}} \approx 3400$.

The angular size of the sound horizon θ_* at the CMB last-scattering is an observable quantity, which can be determined by the location of the first peak in the CMB power spectra. The parameter θ_* is expressed by using the comoving distance $D(z_*)$ and the sound horizon $r_{s,*}$ as

$$\theta_* \equiv \frac{r_{s,*}}{D(z_*)}, \quad (2.5)$$

where $z_* \approx 1090$ is the redshift at the last-scattering surface. The quantities $D(z_*)$ and $r_{s,*}$ depend on the Hubble parameter as

$$D(z_*) = \int_0^{z_*} dz \frac{1}{H}, \quad r_{s,*} = \int_{z_*}^{\infty} dz \frac{c_s(z)}{H}, \quad (2.6)$$

where

$$c_s(z) = \left(1 + \frac{3\Omega_{b,0}h^2}{4\Omega_{\gamma,0}h^2(1+z)} \right)^{-1/2}, \quad (2.7)$$

is the sound speed in the baryon-photon fluid. From Eq. (2.6), we see that $D(z_*)$ and $r_{s,*}$ are determined by the physics after and before the recombination, respectively. For $z \geq z_*$, we can ignore the dark energy density parameter in Eq. (2.3). Thus, using the values of $\Omega_{m,0}h^2$ and $\Omega_{r,0}h^2$ shown above, we get $r_{s,*} = 0.481\bar{H}_0^{-1} \approx 144 \text{ Mpc}$. On the other hand, for $z \leq z_*$, the dark energy density parameter cannot be neglected. In Eq. (2.6), we can eliminate $\Omega_{\Lambda,0}$ with the help of Eq. (2.4) and substitute the determined values for $\Omega_{m,0}h^2$ and $\Omega_{r,0}h^2$. Then, $D(z_*)$ in Eq. (2.6) becomes a function of only h . We find an approximate relation $D(z_*) \approx 3.2/H_0$, and thus Eq. (2.5) implies $H_0 \approx 3.2\theta_*/r_{s,*}$. Therefore, for given θ_* and $r_{s,*}$, we can estimate H_0 . A more precise analysis has been performed using Markov Chain Monte Carlo simulations and gives $H_0 = 67.4 \pm 0.5 \text{ km s}^{-1} \text{ Mpc}^{-1}$ [1].

The approximate relation $H_0 \approx 3.2\theta_*/r_{s,*}$ implies that if $r_{s,*}$ is decreased, an inferred value of H_0 obtained from the CMB observations is increased. In EDE scenario, an additional contribution to the energy density, *i.e.*, EDE, is supposed before the recombination. The EDE decreases $r_{s,*}$ and thus increases H_0 . The scalar energy density $\rho_\phi(z)$ in Eq. (2.2) can be identified as the EDE. To be $D(z_*)$ unchanged, $\rho_\phi(z)/\rho(z) \simeq 0$ should be satisfied for $z < z_*$.

Several possibilities and models related to the origins of the EDE have recently been studied [4]. In the following, we restrict our attention to the cases where the EDE appears through the dynamics of scalar fields in scalar potentials. We denote a homogeneous and canonical scalar field by $\phi(t)$, whose dynamics are determined by the following equation of motion:

$$\ddot{\phi}(t) + 3H(t)\dot{\phi}(t) + \frac{dV(\phi)}{d\phi} = 0, \quad (2.8)$$

where $V(\phi)$ is a scalar potential. The energy density ρ_ϕ and the pressure p_ϕ of ϕ are given by

$$\rho_\phi = \frac{1}{2}\dot{\phi}^2 + V(\phi), \quad p_\phi = \frac{1}{2}\dot{\phi}^2 - V(\phi). \quad (2.9)$$

The time evolution of the energy density of the scalar field is tightly connected to the EoS, which is denoted by $w_\phi = p_\phi/\rho_\phi$. If the potential contribution dominates in the energy density as $\rho_\phi \simeq V(\phi)$ and $w_\phi \simeq -1$, the energy density ρ_ϕ is approximately constant against expansion of the universe, like $\rho_{\Lambda,0}$. On the other hand, if the kinetic energy dominates the energy density as $\rho_\phi \simeq \dot{\phi}^2/2$ and $w_\phi \simeq 1$, ρ_ϕ rapidly decreases as the universe expands.

If ρ_ϕ gives the suitable EDE to resolve the Hubble tension, the time dependence of w_ϕ is restricted. Let us discuss the expected behavior of w_ϕ and the EDE scalar. First, w_ϕ varies around a specific epoch in the history of the universe. We denote the redshift and the time at the epoch by z_{EDE} and t_{EDE} . The precise value of z_{EDE} is model dependent, and $z_* < z_{\text{EDE}} \leq 10^6$ is suggested in the analysis [34]. Let ϕ_{min} be a value of the scalar ϕ that minimizes the potential $V(\phi)$. For $z \gg z_{\text{EDE}}$, to obtain the time dependence of w_ϕ , ϕ must deviate from ϕ_{min} and is frozen or slowly rolling in its potential due to the Hubble friction in Eq. (2.8). We denote the value of the scalar for $z \gg z_{\text{EDE}}$ by ϕ_{ini} . At this epoch, the energy density and the EoS satisfy $\rho_\phi \simeq V(\phi_{\text{ini}}) \equiv V_{\text{ini}}$, and $w_\phi \simeq -1$ holds as the EoS of dark energy. Since ρ_r and ρ_m dominate the energy density of the universe, the contribution from ρ_ϕ is negligible in the universe for $z \gg z_{\text{EDE}}$. As the universe expands, ρ_r and ρ_m decrease, and then ρ_ϕ starts to give a few percent contributions to the total energy density of the universe for $z \simeq z_{\text{EDE}}$. Simultaneously, the scalar field starts to roll down its potential quickly, which is triggered when the Hubble friction in Eq. (2.8) is sufficiently weakened. Thus, around z_{EDE} , the value of the EDE scalar rapidly departs from ϕ_{ini} , and the EoS w_ϕ changes to a positive value. Finally, for $z \ll z_{\text{EDE}}$, $w_\phi > 0$ should be maintained to suppress ρ_ϕ compared to ρ_m .

The above discussion gives constraints on the potential for the EDE scalar ϕ . As stated in Sec. 1, we focus on the periodic potential of the following form:

$$V^{(n)}(\phi) = \Lambda_{(n)}^4 \left(1 + \cos \frac{\phi}{f} \right)^n, \quad (2.10)$$

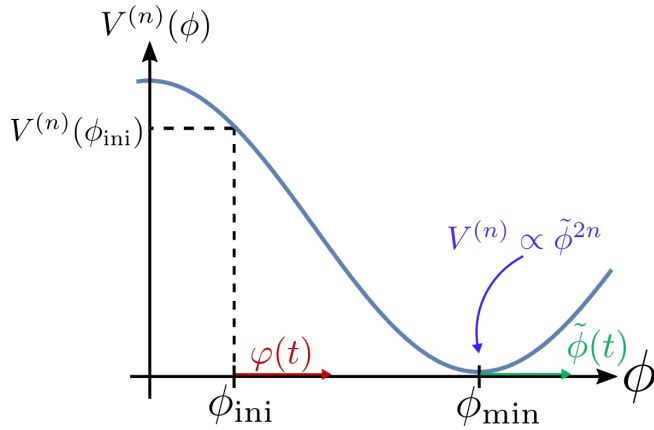


Figure 1: The periodic scalar potential $V^{(n)}(\phi)$ in Eq. (2.10). The EDE scalar $\phi(t)$ is parametrized as $\phi(t) = \phi_{\text{ini}} + \varphi(t)$ for $z \simeq z_{\text{EDE}}$ and as $\phi(t) = \phi_{\text{min}} + \tilde{\phi}(t)$ for $z \ll z_{\text{EDE}}$. Around a minimum, the potential is approximately proportional to $\tilde{\phi}^{2n}$.

where $\Lambda_{(n)}$ and f are parameters with mass dimension one, and $n \geq 1$ is an integer. We refer to Eq. (2.10) as the PNCB potential since the above periodic potential is generally expected to appear for PNCBs, *e.g.*, for axion-like particles. The PNCB potential is considered to be generated by non-perturbative effects such as instanton expansion and interpreted as the result of the spontaneous breakdown of approximate global symmetries. The parameter f corresponds to the energy scale of the symmetry breaking. The scale $\Lambda_{(1)}$ is the dynamical scale generated through non-perturbative effects. For $n \geq 2$, the potential contributions arise from higher-order instanton effects, and $\Lambda_{(n)}/\Lambda_{(1)} \ll 1$ is expected if $\Lambda_{(1)}$ is suppressed than some ultra-violet cutoff scale [53, 54]. While the potential for ϕ generally has the form of $V(\phi) = \sum_n V^{(n)}(\phi)$, the dominant contribution is mostly given by $n = 1$ as $V(\phi) \simeq V^{(1)}(\phi)$. Nevertheless, to keep the discussion general, we consider the case with $V(\phi) \simeq V^{(n)}(\phi)$ even for $n \geq 2$ in the following.

Let us see constraints on the potential (2.10) above. First, we focus on the epoch $z \gg z_{\text{EDE}}$, where the EDE scalar is approximately frozen around ϕ_{ini} , which gives the initial value of the potential by $V^{(n)}(\phi_{\text{ini}}) = C_0^n \Lambda_{(n)}^4$, where $C_0 \equiv 1 + \cos(\phi_{\text{ini}}/f)$. Then, $C_0 \sim \mathcal{O}(1)$ is expected without a fine-tuning of ϕ_{ini} . The energy density of the EDE scalar takes $\rho_\phi \simeq V^{(n)}(\phi_{\text{ini}})$ for $z \gg z_{\text{EDE}}$, and ρ_ϕ should give a few percent contributions to the total energy density around z_{EDE} . Thus, by introducing the numerical parameter $\delta = \mathcal{O}(10^{-2})$, we obtain

$$\delta = \frac{\rho_\phi(z_{\text{EDE}})}{\rho(z_{\text{EDE}})} \simeq \frac{C_0^n \Lambda_{(n)}^4}{3M_{\text{P}}^2 H^2(t_{\text{EDE}})}, \quad (2.11)$$

which constrains the mass scale of the potential.

Next, we consider the dynamics of the EDE scalar around z_{EDE} , where the scalar starts to change its value from ϕ_{ini} . Let us parametrize $\phi = \phi_{\text{ini}} + \varphi$ as shown in Fig. 1 and assume

$|\varphi/f| \ll 1$ for $z \simeq z_{\text{EDE}}$. Then, Eq. (2.8) determines the evolution of φ as

$$3H \frac{\dot{\varphi}}{f} \simeq -\frac{1}{f} \frac{d}{d\phi} V^{(n)}(\phi_{\text{ini}} + \varphi) \simeq nC_0^{n-1} \frac{\Lambda_{(n)}^4}{f^2} \left[-\{(2 - C_0)n - 1\} \frac{\varphi}{f} + \sin \frac{\phi_{\text{ini}}}{f} \right], \quad (2.12)$$

where we have approximately neglected the first term in Eq. (2.8). In addition, we only take the leading order of φ/f in the above last equation. If we parametrize the Hubble parameter as $H(t) = b/t$, where $b = 2/3$ ($1/2$) in the matter-dominated (radiation-dominated) era, the solution of Eq. (2.12) is written as follows:

$$\frac{|\varphi|}{f} \simeq \frac{\sin(\phi_{\text{ini}}/f)}{|(2 - C_0)n - 1|} \left[\exp \left(\frac{nC_0^{n-1} |(2 - C_0)n - 1| \Lambda_{(n)}^4 t^2}{6bf^2} \right) - 1 \right]. \quad (2.13)$$

This solution implies the following relation:

$$H^2(t_{\text{EDE}}) \simeq \frac{bnC_0^{n-1} |(2 - C_0)n - 1| \Lambda_{(n)}^4 f^{-2}}{6}, \quad (2.14)$$

which also constraints the parameters of the potential.

From Eqs. (2.11) and (2.14), we obtain

$$\Lambda_{(n)} \simeq \left(\frac{3\delta}{C_0^n} \right)^{1/4} \sqrt{H(t_{\text{EDE}}) M_{\text{P}}}, \quad f \simeq \left(\frac{3\delta}{C_0^n \tilde{C}} \right)^{1/2} M_{\text{P}}, \quad (2.15)$$

where $\tilde{C} \equiv 6(bnC_0^{n-1} |(2 - C_0)n - 1|)^{-1}$ is a dimensionless parameter. Without fine-tuning of the parameters, C_0 and \tilde{C} in Eq. (2.15) are expected to be $\mathcal{O}(1)$. In addition, $H(t_{\text{EDE}}) \sim 10^{-28}$ eV is satisfied for $z_{\text{EDE}} \sim 4000$, which is an example and a typical value. Thus, the parameters in the PNCB potential in Eq. (2.10) should satisfy $\Lambda_{(n)} \sim 1$ eV and $f \sim M_{\text{P}}$ in the EDE scenario. This result is not sensitive to a precise value of z_{EDE} .

Finally, we consider the dynamics of the EDE scalar for $z < z_{\text{EDE}}$. The scalar begins to evolve to a minimum of the potential in Eq. (2.10) around z_{EDE} and then rapidly oscillates around the minimum. Let $\tilde{\phi}$ be a fluctuation of the scalar from the minimum as shown in Fig. 1. For $z \ll z_{\text{EDE}}$, Eq. (2.10) implies that $\tilde{\phi}$ oscillates in the following polynomial potential:

$$V^{(n)}(\tilde{\phi}) \simeq \frac{\Lambda_{(n)}^4}{2^n} \left(\frac{\tilde{\phi}}{f} \right)^{2n}. \quad (2.16)$$

The period of the oscillation is characterized by the time scale of $\mathcal{O}(1/H(z_{\text{EDE}}))$, and the EoS of the scalar also oscillates for $z \ll z_{\text{EDE}}$. Due to the Hubble friction term in Eq. (2.8), the oscillation amplitude decreases with a time scale, which is much longer than the oscillation period. In this case, the time-averaged value of the EoS $\langle w_\phi(z) \rangle$ is approximately given by [47]

$$\langle w_\phi(z) \rangle \simeq \frac{n-1}{n+1}, \quad \text{for } z \ll z_{\text{EDE}}. \quad (2.17)$$

Therefore, to decrease the energy density ρ_ϕ faster than ρ_m , $n \geq 2$ is required [34]. In the $n = 2$ case, $\langle w_\phi(z) \rangle \simeq 1/3$ holds during the oscillation, and ρ_ϕ behaves like ρ_r . Thus, the EDE scenario with the $n = 2$ potential and models with extra radiation components, which modify N_{eff} [1, 55–57], are partly degenerate in their predictions. A novel and the minimal setting is the $n = 3$ case, which is suggested to be the most effective to the Hubble tension in the analysis in [30].

We summarize the discussion in this section. We focus on the EDE scenario in which the scalar dynamics in the PNGB potential (2.10) explain the time evolution of the EDE. The mass parameters in Eq. (2.10) are constrained as $\Lambda_{(n)} \sim 1$ eV and $f \sim M_{\text{P}}$. In addition, the leading potential must be $n \geq 2$ contributions to obtain a sufficient suppression of the EDE for $z \ll z_{\text{EDE}}$. The vast hierarchy in the potential parameters implies an underlying mechanism that controls the potential. Ultralight axions can have potentials with hierarchical mass scales [54], and they are considered to be a candidate for the EDE scalar [30, 31, 34]. However, as noted above, the PNGB potential is expected to be dominated by the $n = 1$ contribution, which is inadequate for the EDE scenario. Thus, if an axion-like particle is identified as the EDE scalar, an unknown mechanism, which ensures that $n \geq 2$ contributions dominate the potential, is required. In this paper, as an alternative to the axion case, we point out that the scalar potential suitable to the EDE scenario appears in models incorporating a compact extra dimension. As seen below, an extra-dimensional component of gauge fields naturally has a potential adequate to the EDE scalar through quantum corrections.

3 Higher-dimensional gauge field as the EDE scalar

As discussed in the previous section, the potential for the EDE scalar should satisfy severe constraints to solve the Hubble tension. Since there is no candidate for the EDE scalar among the known particles in nature, physics beyond the SM is implied to explain the EDE scalar. Although we can introduce a scalar field and fix the scalar potential by hand, it needs extreme fine-tuning; this is because scalar potentials generally receive quantum corrections, and the potential energy tends to be comparable to an ultraviolet cutoff scale. Thus, we should address the problem of revealing the underlying physics of the EDE scalar from the particle physics viewpoint.

Here, we discuss the possibility that the EDE scalar naturally emerges from higher-dimensional gauge theories, which are well-motivated candidates for physics beyond the SM. In these theories, there are higher-dimensional components of gauge fields, which are regarded as 4D scalar fields at low energy, and may be identified as the EDE scalar. The gauge invariance strictly restricts their potentials, and as examined below, we can obtain the effective potential, which is adequate to EDE resolution to the Hubble tension, without fine-tuning in higher-dimensional gauge theories.

As concrete examples, let us discuss the extra-dimensional models based on a five-dimensional (5D) $U(1)$ gauge theory, where 5D spacetime consists of the Minkowski spacetime and a compact space. In the following, we assume for simplicity that the gauge

group, which we denote by $U(1)_D$, is the gauge symmetry for a dark sector. Namely, the SM fields, such as baryons and leptons, are neutral under the $U(1)_D$ symmetry. We denote the spacetime coordinates by x^M ($M = 0, 1, 2, 3, 5$); we also use x^μ ($\mu = 0, 1, 2, 3$) and $y = x^5$. The geometry of the compact extra space is assumed to be a circle S^1 or an orbifold S^1/\mathbb{Z}_2 . In both cases, we denote the radius of S^1 by R . Thus, for the S^1 compactification, we demand the identification $y \sim y + 2\pi R$. For the S^1/\mathbb{Z}_2 compactification, the extra identification $y \sim -y$ is also imposed.

In the 5D gauge theory, the gauge field is denoted by $A_M = (A_\mu, A_5)$. As matter fields for the dark sector, we introduce N_f and N_b flavors of 5D fermion fields ψ_m ($m = 1, \dots, N_f$) and complex scalar fields ϕ_m ($m = 1, \dots, N_b$), respectively. The matter fields are assumed to be charged under the $U(1)_D$ and neutral under the SM gauge symmetry. The action and the Lagrangian density of the dark sector is written as follows:

$$S = \int d^4x \int_0^{2\pi R} dy (\mathcal{L}_g + \mathcal{L}_\varphi), \quad (3.1)$$

$$\mathcal{L}_g = -\frac{1}{4} F_{MN} F^{MN}, \quad F_{MN} = \partial_M A_N - \partial_N A_M, \quad (3.2)$$

$$\mathcal{L}_\varphi = \sum_{m=1}^{N_f} \bar{\psi}_m (i\Gamma^M D_M - M_{\psi_m}) \psi_m + \sum_{m=1}^{N_b} [|D_M \phi_m|^2 - M_{\phi_m}^2 |\phi_m|^2], \quad (3.3)$$

where M_φ ($\varphi = \psi_m, \phi_m$) are bulk mass parameters and $\Gamma^M = (\gamma^\mu, i\gamma^5)$ are the 5D gamma matrices. The covariant derivative D_M is given by $D_M = \partial_M - ig_D q_\varphi A_M$, where g_D is the gauge coupling and q_φ ($\varphi = \psi_m, \phi_m$) is a $U(1)_D$ charge of φ . The Lagrangian density is invariant under the following gauge transformation:

$$A_M \rightarrow A_M + \frac{1}{g_D} \partial_M \Lambda, \quad \varphi \rightarrow e^{iq_\varphi \Lambda} \varphi, \quad (\varphi = \psi_m, \phi_m). \quad (3.4)$$

At an energy scale below the compactification scale $1/R$, the effective 4D description is valid, where a five-dimensional field is expanded as infinite towers of Kalzua-Klein (KK) modes that only depend on the 4D coordinates. Except for zero-modes, whose wave functions are completely flat along the extra dimension, the KK modes have large masses of $\mathcal{O}(1/R)$ at the classical level. We suppose that $1/R$ is much larger than the typical energy scale of the EDE scalar potential. Thus, we focus on the case where A_5 has a zero-mode.

The KK expansion is determined by boundary conditions, which relate the field values at (x^μ, y) and (x^μ, y') under the identification $y \sim y'$. The boundary conditions can be chosen such that the Lagrangian densities at (x^μ, y) and (x^μ, y') have the same value [58]. To obtain an A_5 zero-mode, one can introduce the boundary condition $A_M(x^\mu, y + 2\pi R) = A_M(x^\mu, y)$ for the S^1 compactification. In this case, both A_μ and A_5 have zero-modes. On the other hand, for the S^1/\mathbb{Z}_2 compactification, there is an additional boundary condition associated with the identification $y \sim -y$. Under the parity transformation of the fifth dimension, $y \rightarrow -y$, A_5 changes its sign. Thus, in the S^1/\mathbb{Z}_2 case, we cannot take common boundary conditions for A_μ and A_5 . To obtain an A_5 zero-mode, we can consistently introduce the additional boundary

conditions as $A_\mu(x, -y) = -A_\mu(x, y)$ and $A_5(x, -y) = A_5(x, y)$. These boundary conditions are related to the outer automorphism, which is the complex conjugation of the representation of $U(1)_D$, and are called the conjugate boundary condition [59–61]. In this case, while A_5 has its zero-mode, A_μ does not have, and the $U(1)_D$ gauge symmetry is broken.

In these cases, the A_5 zero-mode can be identified as the EDE scalar. Hereafter, we denote the A_5 zero-mode by $A_5^{(0)}$. The canonical normalization of $A_5^{(0)}$ implies $A_5 \ni A_5^{(0)}/\sqrt{2\pi R}$, and the effective 4D gauge coupling \tilde{g}_D is given by $\tilde{g}_D = g_D/\sqrt{2\pi R}$.

For the matter fields, boundary conditions should also be considered. For the S^1 case, we impose $\varphi(x^\mu, y + 2\pi R) = e^{i\eta_\varphi}\varphi(x^\mu, y)$ ($\varphi = \phi_m, \psi_m$), where $\eta_\varphi \in \mathbb{R}$ is a parameter. For the S^1/\mathbb{Z}_2 case, we introduce the additional conditions as $\phi_m(x^\mu, -y) = \phi_m^*(x^\mu, y)$ and $\psi_m(x^\mu, -y) = i\psi_m^c(x^\mu, y)$, where c denotes the charge conjugation of the 4D Dirac fermion. In both cases, the bulk mass terms for the matter fields in Eq. (3.3) are invariant under the boundary conditions.³

Let us discuss the potential for $A_5^{(0)}$. The gauge field has a flat potential at the classical level, and an effective potential is radiatively generated. We denote a homogeneous background value by $\langle A_5^{(0)} \rangle$. Note that $\langle A_5^{(0)} \rangle$ is gauge dependent since gauge transformations in Eq. (3.4) change the background value. The Wilson line defined with a non-contractible loop along the compact extra-dimension is a gauge-invariant quantity and has physical consequences in the present setup. The background value of the Wilson line W is written as

$$\langle W \rangle = e^{ig_D \int_0^{2\pi R} dy \langle A_5 \rangle} = e^{2\pi i R \tilde{g}_D \langle A_5^{(0)} \rangle} = e^{i\theta_5}, \quad (3.5)$$

where we have defined the phase parameter $\theta_5 = 2\pi R \tilde{g}_D \langle A_5^{(0)} \rangle$ and taken the minimum unit of $U(1)_D$ charge to be 1. Due to the phase property of the Wilson line, the effective potential for $\langle A_5^{(0)} \rangle$ is given by a periodic function of θ_5 , *i.e.*, $V(\theta_5) = V(\theta_5 + 2\pi n)$ ($n \in \mathbb{Z}$). If a matter field φ having a bulk mass M_φ exists, the following contribution to the effective potential $V(\theta_5)$ is generated at the one-loop level [62, 63]:

$$\Delta V_\varphi(\theta_5) = \frac{3n_\varphi M_c^4}{4\pi^2} \sum_{\ell=1}^{\infty} e^{-\ell M_\varphi/M_c} \left[\frac{1}{\ell^5} + \frac{1}{\ell^4} \frac{M_\varphi}{M_c} + \frac{1}{3\ell^3} \frac{M_\varphi^2}{M_c^2} \right] \cos[\ell(q_\varphi \theta_5 - \eta_\varphi)], \quad (3.6)$$

where we have defined $M_c = (2\pi R)^{-1}$. The factor n_φ takes 4 (−2) if φ is a 5D fermion (complex scalar) for the S^1 case, whereas n_φ takes 2 (−1) for the S^1/\mathbb{Z}_2 case. In general, there is a constant contribution to the potential, which is ignored in Eq. (3.6) and can be canceled by a constant dark energy. Also, additional contributions to $V(\theta_5)$ can arise through 5D gravitational interactions, which may be large and change the potential structure in Eq. (3.6). However, if $M_c/M_5 < 1$ is satisfied, where M_5 is the 5D Planck mass parameter, such quantum gravity corrections are safely neglected [48]. Thus, we consider the case with $M_c/M_5 < 1$. The one-loop effective potential for θ_5 is given by the sum of the contributions from the matter fields in the model, *i.e.*, $V(\theta_5) = \sum_\varphi \Delta V_\varphi(\theta_5)$.

³In S^1/\mathbb{Z}_2 case, depending on boundary conditions, we should incorporate a pair of fermions with opposite \mathbb{Z}_2 parities to construct invariant mass terms under the boundary conditions [63].

From Eq. (3.6), if $M_\varphi/M_c > 1$ is satisfied, we find that the potential contribution is approximately written by

$$\Delta V_\varphi(\theta_5) \simeq \frac{n_\varphi M_\varphi^2 M_c^2}{4\pi^2} e^{-M_\varphi/M_c} \cos(q_\varphi \theta_5 - \eta_\varphi). \quad (3.7)$$

In this case, the potential is given by the simple cosine form as the PNCB potential in Eq. (2.10), and the exponential factor in Eq. (3.7) strongly suppresses the energy scale of the potential compared to $\sqrt{M_\varphi M_c}$. This suppression reflects the non-locality of the Wilson line phase degrees of freedom. Since the potential contributions can be seen as the result of virtual propagations of the massive matter fields along non-contractible cycles, the contribution scales like $e^{-2\pi R \ell M_\varphi}$. Thus, if $M_\varphi/M_c > 1$ is satisfied, we can naturally obtain a suitable EDE scale through the potential in Eq. (3.7) with a wide parameter range of the compactification scale M_c .

Based on the above discussions, we study the constraints for the mass parameters in the scenario where the EDE scalar is the extra-dimensional gauge field. To obtain the PNCB-like potential (3.7) for the EDE scalar, the condition,

$$M_c < M_\varphi < M_5, \quad (3.8)$$

should be satisfied. Since the 4D Planck mass M_P is given by the 5D Planck mass M_5 and the compactification scale M_c as $M_5^3 = M_c M_P^2$, we can rewrite the condition (3.8) as

$$1 < \frac{M_\varphi}{M_c} < \left(\frac{M_P}{M_c}\right)^{2/3}. \quad (3.9)$$

In Fig. 2, we show the allowed range of the parameters in this scenario, where the blue (red) shaded region is not consistent with the first (second) inequality in Eq. (3.9).

Let us examine the typical parameters that give the required energy scale for EDE. As discussed in Sec. 2, if the EDE scalar potential is given by Eq. (2.10), $\Lambda_{(n)} \sim 1$ eV and $f \sim M_P$ should be satisfied. In the present case, a similar discussion gives the following constraints:

$$\frac{M_\varphi^2 M_c^2}{4\pi^2} e^{-M_\varphi/M_c} \sim (1 \text{ eV})^4, \quad \frac{M_c}{\tilde{g}_D} \sim M_P, \quad (3.10)$$

where we have ignored $\mathcal{O}(1)$ factors such as n_φ and q_φ . Typical values of M_φ/M_c that satisfy the constraints in Eq. (3.10) are given by the solutions of the following equation:

$$\frac{M_\varphi}{M_c} = -2W_k \left(-\frac{10^{-54}}{2} \left(\frac{M_c}{M_P}\right)^{-2} \right), \quad (3.11)$$

where W_k ($k = -1, 0$) is the Lambert W function. For a given $M_c/M_P \geq 10^{-27}e/2$, where $e = 2.71828\dots$, there are two solutions of Eq. (3.11), which we denote in Fig. 2 as the solid and the dashed lines. As seen from the figure, only the solution of the $k = -1$ case of Eq. (3.11) is consistent with the constraint in Eq. (3.8).

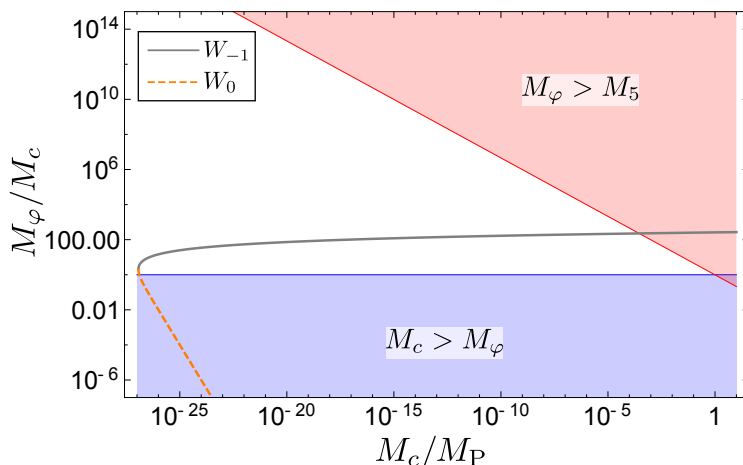


Figure 2: The allowed range of the mass parameters in the scenario where the extra-dimensional gauge field is identified as the EDE scalar. The blue shaded region is inconsistent with the first inequality in Eq. (3.9), where a PNCB-like potential (3.7) with a suppressed energy scale suitable for the EDE scalar potential cannot be obtained. The red shaded region is inconsistent with the second inequality in Eq. (3.9), where the gravitational corrections to the potential are not safely neglected. The solid (black) and dashed (red) lines correspond to the solution of Eq. (3.11) for a given M_c/M_P .

From the above analysis, we find that a wide range of the compactification scale is allowed for the present scenario with $M_c/M_P \lesssim 10^{-3}$. The ratio between the bulk mass scale for matter fields and M_c should satisfy $M_\varphi/M_c \sim \mathcal{O}(100)$. The $\ell \geq 2$ terms in the effective potential (3.7) are consistently neglected with the typical values of M_φ/M_c . Note that the second relation in Eq. (3.10) implies that the required value of the 4D gauge coupling constant \tilde{g}_D is determined by M_c/M_P , which is $\tilde{g}_D \lesssim 10^{-3}$ in the allowed region. Such a small value of \tilde{g}_D is consistent with the perturbative evaluation and the one-loop approximation of the effective potential in Eq. (3.6).

In this section, we have studied the scenario where the 5D component of the gauge field A_5 in a 5D dark sector is identified as the EDE scalar. The compactification scale of the extra dimension M_c is smaller than $\mathcal{O}(10^{-3}M_P)$. The effective 4D gauge coupling in the dark sector \tilde{g}_D is predicted to be comparable to M_c/M_P . If a bulk mass for a matter field satisfies $M_\varphi/M_c \sim \mathcal{O}(100)$, the effective potential for A_5 is sufficiently suppressed to give the tiny energy scale of the EDE scalar potential without extreme fine-tuning of the parameters. In addition to these conditions, to obtain realistic EDE potentials, EDE should decrease faster than the matter energy density in the late universe. As discussed in Sec. 2, such late-time behavior of EDE is described by $n \geq 2$ potential of Eq. (2.16) around its minimum. As we will see, A_5 potentials also explain the late-time behavior of EDE if there are both fermions and scalars as the bulk matter fields in the dark sector.

4 Explicit examples of 5D $U(1)_D$ EDE models

In this section, we show examples of 5D $U(1)_D$ models that give EDE. For simplicity of the discussion, we assume that the bulk matter fields satisfy the periodic boundary conditions, *i.e.*, $\eta_\varphi = 0$, and have a degenerate bulk mass as $M_\varphi = M$. In this case, the effective potential for θ_5 is written by

$$\begin{aligned} V_{\text{eff}}(\theta_5) &= -V_0 \sum_{\varphi} n_{\varphi} [1 - \cos(q_{\varphi}\theta_5)], \\ V_0 &= \frac{M^2 M_c^2}{4\pi^2} e^{-M/M_c}, \end{aligned} \quad (4.1)$$

where we have added a constant contribution to the potential in order to simplify the following discussion. We hereafter refer to θ_5 as the EDE phase.

If we specify the matter contents of the model, the effective potential in Eq. (4.1) is determined. As seen in Sec. 2, if an EDE scalar oscillates around a minimum of $n \geq 2$ potential in Eq. (2.16), EDE dilutes sufficiently faster than the matter energy density in the late universe. Such dilution can be ensured in our setup by specific bulk matter contents. To see this, we focus on the late-time behavior of the EDE phase, which is assumed to oscillate around $\theta_5 = 0$ in the potential. For $|\theta_5| \ll 1$, the potential is approximately written as

$$V_{\text{eff}}(\theta_5) \simeq V_0 \sum_{k=1}^{\infty} \frac{(-1)^k}{2k!} \left(\sum_{\varphi} n_{\varphi} q_{\varphi}^{2k} \right) \theta_5^{2k}. \quad (4.2)$$

Let us define

$$V_{\text{eff}}^{(n)}(\theta_5) \equiv V_0 \left(\sum_{\varphi} n_{\varphi} q_{\varphi}^{2n} \right) \frac{(-1)^n}{2n!} \theta_5^{2n} + \mathcal{O}(\theta_5^{2n+2}). \quad (4.3)$$

Thus, if $V_{\text{eff}}(\theta_5) \simeq V_{\text{eff}}^{(n)}(\theta_5)$ is satisfied for $|\theta_5| \ll 1$, the EoS of the EDE phase is given by the same form as Eq. (2.17). For $n \geq 2$, EDE dilutes faster than the matter energy density.

To obtain $V_{\text{eff}}(\theta_5) \simeq V_{\text{eff}}^{(n)}(\theta_5)$, bulk matter contents are restricted, and the parameters related to the matter contents should satisfy

$$\sum_{\varphi} n_{\varphi} q_{\varphi}^{2k} = 0, \quad \text{for } k = 1, \dots, n-1. \quad (4.4)$$

For a given set of fields φ with charge q_{φ} , we can regard Eq. (4.4) as constraints for n_{φ} . If there are equal to or more than n kinds of fields with different $U(1)_D$ charges, there exist solutions of n_{φ} in Eq. (4.4) as shown in Appendix A.

We show an explicit example of models that give $V_{\text{eff}}(\theta_5) \simeq V_{\text{eff}}^{(n)}(\theta_5)$. Let us express bulk scalars or fermions whose $U(1)_D$ charges are q_i by φ_i ($i = 1, \dots, n$), where $|q_i| \neq |q_j|$ for $i \neq j$.

In addition, let $|d_i|$ be the sum of the degrees of freedom of φ_i , where $d_i < 0$ ($d_i > 0$) for scalars (fermions). In this case, the solution of the constraint (4.4) is given by

$$\frac{d_i}{d_j} = -\frac{q_j^2}{q_i^2} \prod_{\substack{k=1 \\ k \neq i, j}}^n \frac{q_j^2 - q_k^2}{q_i^2 - q_k^2}, \quad (4.5)$$

for $i \neq j$. The effective potential is approximately written as follows:

$$V_{\text{eff}}(\theta_5) \simeq V_{\text{eff}}^{(n)}(\theta_5) = -\frac{V_0}{(2n)!} d_j q_j^2 \left(\prod_{\substack{k=1 \\ k \neq j}}^n (q_k^2 - q_j^2) \right) \theta_5^{2n} + \mathcal{O}(\theta_5^{2n+2}), \quad (4.6)$$

which holds for any j .

For example, $V_{\text{eff}}(\theta_5) \simeq V_{\text{eff}}^{(2)}(\theta_5)$ is given by the bulk matter content consisting of eight complex scalars with charge q_1 and a 5D fermion with $q_2 = 2q_1$ or $-2q_1$. We refer to the above case as the $n = 2$ model hereafter. Also, the $n = 3$ model is defined by, *e.g.*, the bulk matter content consisting of 15 complex scalars with charge q_1 , a complex scalar with charge $q_2 = 3q_1$ or $-3q_1$, and three 5D fermions with charge $q_3 = 2q_1$ or $-2q_1$.⁴ The required bulk matter contents and $U(1)$ charges for $n \geq 2$ models can be given by hand and regarded as a setup. Also, a suitable matter sector may be realized more naturally through underlying mechanisms such as flavor symmetries.

With the above specific matter contents, let us discuss the time evolution of the EDE phase and its energy density. In a 4D low-energy effective theory, $\langle A_5^{(0)} \rangle$ is a canonically normalized scalar field, which obeys the following equation of motion:

$$\langle \ddot{A}_5^{(0)} \rangle + 3H(t) \langle \dot{A}_5^{(0)} \rangle + 2\pi R \tilde{g}_D \frac{dV_{\text{eff}}(\theta_5)}{d\theta_5} = 0. \quad (4.7)$$

Let w_{θ_5} and ρ_{θ_5} be the EoS and the energy density of the EDE phase, respectively. In addition, we denote the energy density parameter of θ_5 by Ω_{θ_5} , which is the ratio between ρ_{θ_5} and the total energy density of the universe. If the potential behaves as $V_{\text{eff}}(\theta_5) \simeq V_{\text{eff}}^{(n)}(\theta_5)$, the time average of w_{θ_5} after a fast-roll period is well approximated by the right-hand side in Eq. (2.17).

For fixed matter contents and a compactification scale M_c , the time evolution of the EDE phase depends on \tilde{g}_D and M . The latter controls the energy scale of $V_{\text{eff}}(\theta_5)$ as understood from Eq. (4.1). On the other hand, \tilde{g}_D is irrelevant to the potential and affects the equation of motion (4.7). As discussed in Sec. 2, θ_5 is initially frozen in its potential. Then, the Hubble friction in Eq. (4.7) becomes sufficiently small, and θ_5 starts to roll down the potential. If \tilde{g}_D is increased (decreased) for a given potential, the effect of the Hubble friction term is diminished (enhanced). Thus, \tilde{g}_D controls the time when the fast roll starts.

⁴If we assume the anti-periodic boundary condition for fermions and scalars, the right-hand side of Eq. (4.1) is multiplied by -1 with a suitable constant shift of the potential. In that case, *e.g.*, $V_{\text{eff}}(\theta_5) \simeq V_{\text{eff}}^{(2)}(\theta_5)$ is given by the bulk matter content consisting of two 5D fermions with charge q_1 and a complex scalar with charge $q_2 = 2q_1$ or $-2q_1$.

Table 1: The parameters and initial conditions for the EDE phase used in the numerical analysis. The predicted value of the 4D gauge coupling constant is also shown.

model	M_c/M_P	M/M_c	\tilde{g}_D	$\theta_5(t_0)$	$\dot{\theta}_5(t_0)$
$n = 2$	1.0×10^{-6}	212.5	6.95×10^{-6}	$\pi/2$	0
$n = 3$	1.0×10^{-6}	213.1	5.00×10^{-6}	$\pi/2$	0

To examine typical dynamics of the EDE phase, we numerically solve the equation of motion of the EDE phase in the $n = 2$ and 3 models. We set $q_1 = 1$ and initialize the system at $t = t_0$, where $z(t_0) = 10^{42}$. Since EDE accounts for less than several percent of the total energy of the universe, the expansion rate of the universe is almost determined by the evolution of the other ingredients. In the following analysis, we consider a universe in the matter-dominant stage, *i.e.*, the Hubble parameter scales as $H(t) = 2/(3t)$ to simplify calculations. For $z \lesssim z_{\text{eq}}$, our universe is well approximated by this treatment. In addition, from the discussion given in Sec. 2, we see that the dynamics of the EDE phase is not sensitive to the value of b under the parametrization $H(t) = b/t$. While EDE may generally become non-negligible during the radiation-dominated period, where $H(t) = 1/(2t)$ holds, or at the matter-radiation equality time, our treatment is sufficient to understand the qualitative behavior of the EDE phase.

To compare the $n = 2$ and 3 models, we choose the parameters such that the fast-roll of the EDE phase begins at almost the same time in each model. In addition, we set similar maximum values of the EDE density parameters for both cases. These conditions fix the values of M/M_P and \tilde{g}_D . The parameters and initial conditions for the EDE phase used in the following analysis are shown in Table 1.

On the left of Fig. 3, we show the normalized effective potential $\bar{V}_{\text{eff}}(\theta_5)$, whose maximal value is one. The dashed (solid) line represents the potential in the $n = 2$ ($n = 3$) model. Around $\theta_5 = 0$, the potential is approximately written as the polynomial form $V_{\text{eff}}(\theta_5) \simeq V_{\text{eff}}^{(n)}(\theta_5) \propto \theta_5^{2n}$. We see that the slope of the potential around the minima is much flatter in the $n = 3$ case. On the right of Fig. 3, we also show the time evolution's of θ_5 in the $n = 2$ and $n = 3$ models by dashed and solid lines. For $z \gtrsim 4000$, θ_5 is frozen in its potential due to the Hubble friction. For $z \sim 4000$, θ_5 starts to roll down in its potential and then oscillates around $\theta_5 = 0$. We see that the oscillation period in the $n = 3$ case is much longer than the one in the $n = 2$ case, as expected from the potential forms.

In Fig. 4, the EoS and the energy density parameter of the EDE phase are shown. From the left in Fig. 4, we see that the EoS w_{θ_5} also starts to oscillate when the EDE phase begins to oscillate around the minimum of the potential. For the $n = 3$ case, the EoS keeps $w_{\theta_5} \simeq 1$ relatively longer than in the $n = 2$ case, as expected from the approximate formula in Eq. (2.17). From the right in Fig. 4, we see that the EDE gives a few percent contribution to the total energy density of the universe around $z = 4000$. Before $z \sim 4000$, ρ_{θ_5} decays more slowly than the background matter and radiation energy densities, as understood by $w_{\theta_5} < w_m < w_r$. Then, around $z = 4000$, the fast-roll of the EDE phase starts and triggers to change the EoS as $\langle w_{\theta_5} \rangle > 0$. Thus, the EDE quickly dilutes after $z \sim 4000$. For the $n = 3$

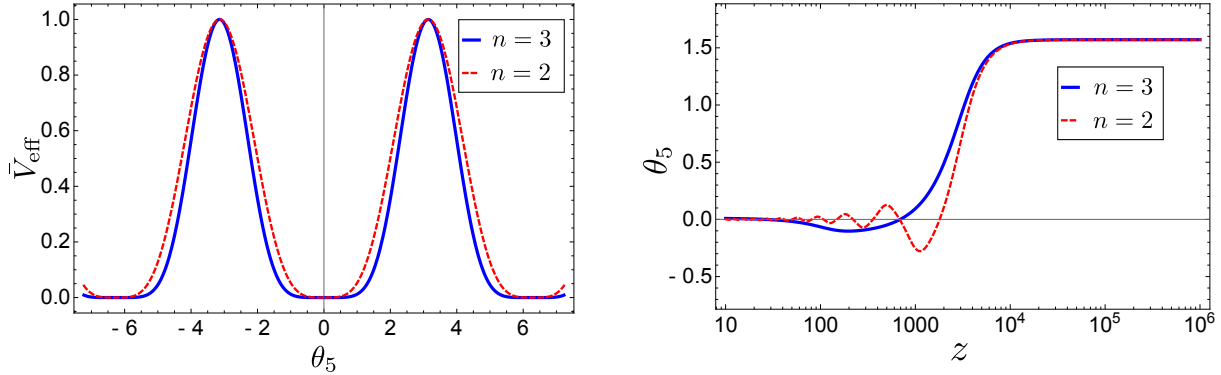


Figure 3: The effective potential for θ_5 (left) and the time evolution of θ_5 as functions of the redshift (right). Here, the shown potential is normalized as $\bar{V}_{\text{eff}}(\theta_5) = V_{\text{eff}}(\theta_5)/V_{\text{eff}}(\pi)$. The dashed (solid) line represents the $n = 2$ ($n = 3$) case. The left figure shows that the flatness of the potential is obtained around $\theta_5 = 0$, where the potential is approximately written as $V_{\text{eff}}(\theta_5) \simeq V_{\text{eff}}^{(n)}(\theta_5) \propto \theta_5^{2n}$. The right figure shows that θ_5 is frozen in the potential for $z \gtrsim 4000$ due to the Hubble friction. For $z \sim 4000$, θ_5 begins fast-roll in its potential and finally oscillates around the potential minimum.

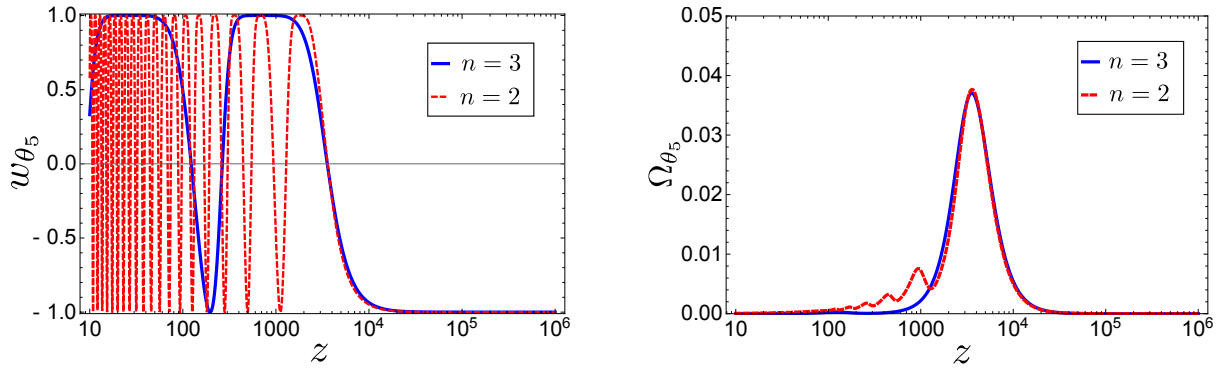


Figure 4: The EoS w_{θ_5} (left) and the energy density parameter Ω_{θ_5} (right) as functions of the redshift. The dashed (solid) line represents the $n = 2$ ($n = 3$) case. For $z \gtrsim 4000$, $w_{\theta_5} \simeq -1$ holds like the dark energy. When θ_5 starts to oscillate, w_{θ_5} also oscillates such that the $w_{\theta_5} > 0$ period is more extended than the $w_{\theta_5} < 0$ one. Thus, the time-averaged value of w_{θ_5} satisfies $\langle w_{\theta_5} \rangle > 0$. For $z > 4000$, as $w_{\theta_5} \simeq -1$ is satisfied, Ω_{θ_5} decays more slowly than the background matter energy density parameter. For $z < 4000$, since the EoS takes $\langle w_{\theta_5} \rangle > 0$, Ω_{θ_5} proceeds to dilute. As seen from the figure, the dilution is more efficient for the $n = 3$ case.

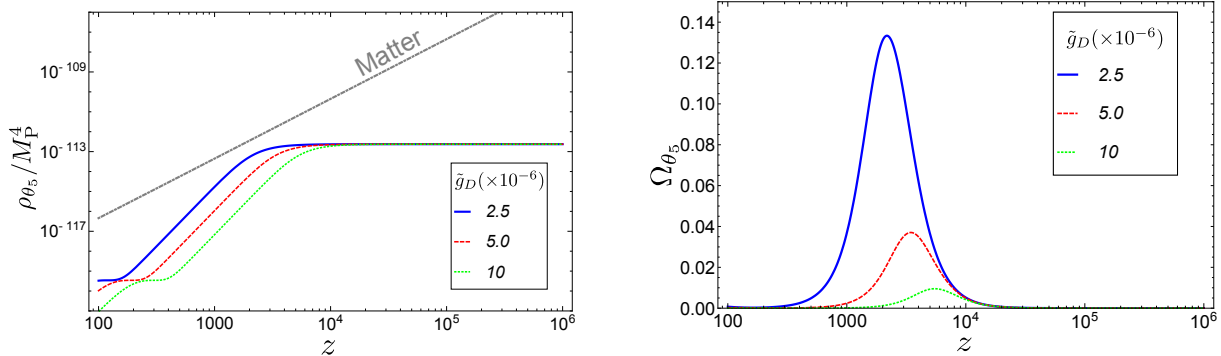


Figure 5: The \tilde{g}_D dependence of the energy density ρ_{θ_5} (left) and the energy density parameter Ω_{θ_5} (right). We take the other parameters as the $n = 3$ case in Table 1. If \tilde{g}_D is increased, the fast-roll of θ_5 starts more earlier, and the peak value of the energy density, Ω_{\max} , is suppressed.

case, dilution is much faster than the one in the $n = 2$ case, as expected from the behavior of the EoS.

Let us discuss the parameter dependence of the EDE properties in our model. The general discussion in Sec. 2 is useful for understanding the parameter dependence. From Eq. (2.15), we see that $f \sim \delta^{1/2} M_P$ holds, where f and δ are defined in Eqs. (2.10) and (2.11). In our scenario, δ corresponds to a maximum value of $\Omega_{\theta_5}(z)$, which we denote by Ω_{\max} . In addition, from the definition of the Wilson line phase, $\theta_5 = \tilde{g}_D M_c^{-1} \langle A_5^{(0)} \rangle$, we realize $f \sim \tilde{g}_D^{-1} M_c$. Thus, we expect that a relation $\Omega_{\max} \sim \tilde{g}_D^{-2} M_c^2 / M_P^2$ is satisfied in our scenario.

To clarify the parameter dependence, we numerically study the $n = 3$ model in more detail. On the left in Fig. 5, we show how the energy density ρ_{θ_5} depends on the coupling constant \tilde{g}_D . As explained, the equation of motion (4.7) depends on \tilde{g}_D , whereas the magnitude of the potential $V_{\text{eff}}(\phi_5)$ does not. Thus, the energy density before $z \sim 4000$ is unchanged even if we vary \tilde{g}_D . On the other hand, z_{\max} , which we define by $\Omega_{\max} = \Omega_{\theta_5}(z_{\max})$, depends on \tilde{g}_D . If \tilde{g}_D is increased, z_{\max} is also increased, and the fast-roll of θ_5 starts earlier. On the right in Fig. 5, we show how the energy density parameter Ω_{θ_5} depends on the coupling constant \tilde{g}_D . Since the energy density of non-relativistic matter ρ_m decays at a constant rate, if \tilde{g}_D is increased, $\Omega_{\theta_5}(z_{\max})$ is decreased.

On the left and right in Fig. 6, we show how ρ_{θ_5} and Ω_{θ_5} depend on the bulk mass parameter M , which affects the size of the potential $V_{\text{eff}}(\theta_5)$. From Eq. (4.1), we see that a larger M suppresses the potential. As a result, if we increase M , both the energy density before $z \sim 4000$ and at z_{\max} are decreased. On the other hand, the maximum value of the energy density parameter is determined by \tilde{g}_D , M_c , and M_P , as explained. Thus, Ω_{\max} does not depend on M as shown in the figure.

In Fig. 7, we show predicted values of z_{\max} and Ω_{\max} as functions of \tilde{g}_D and M . Suppressed values of the coupling constant and bulk mass increase both z_{\max} and Ω_{\max} . If precise constraints on z_{\max} and Ω_{\max} are obtained from future measurements, we may find implications for the fundamental parameters \tilde{g}_D and M/M_c in our model by using the relation shown in

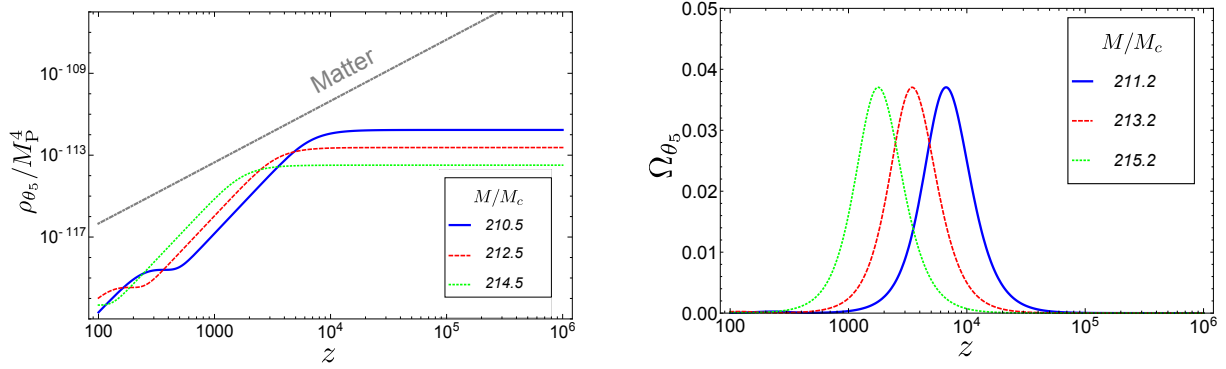


Figure 6: The bulk mass M dependence of the energy density ρ_{θ_5} (left) and the energy density parameter Ω_{θ_5} (right). We take the other parameters as the $n = 3$ case in Table 1. If M is increased, z_{\max} is reduced, while Ω_{\max} is unchanged.

Fig. 7. Note that, in a region where Ω_{\max} takes a relatively large value, the approximation used in the calculation may be worse because only ρ_m is taken into account as the background energy for solving the Friedmann equation. To obtain a more accurate result, a complete treatment of the Friedmann equation is required, which is left for future work.

We can estimate the H_0 value predicted in this scenario by evaluating the sound horizon. Since the difference in $D(z_*)$ between Λ CDM and EDE model is tiny and negligible, the ratio of the Hubble constants of these models is given by

$$\frac{H_0^{\text{EDE}}}{H_0^{\Lambda\text{CDM}}} = \frac{r_{s,*}^{\Lambda\text{CDM}}}{r_{s,*}^{\text{EDE}}}, \quad (4.8)$$

where H_0^x and $r_{s,*}^x$ ($x = \Lambda\text{CDM}, \text{EDE}$) denotes the Hubble constant and the sound horizon in each model. In Sec. 2, we obtained $r_{s,*}^{\Lambda\text{CDM}} = 144$ Mpc from Eq. (2.6) and the *Planck* results. We can calculate $r_{s,*}^{\text{EDE}}$ by adding the energy density of θ_5 to the energy density in Eq. (2.3). In the calculations of $r_{s,*}^{\text{EDE}}$, to include the effects from radiation properly, we use the relation

$$t(z) = \frac{2}{3\bar{H}_0} \frac{1}{\Omega_{m,0}h^2} \left[\frac{1}{1+z} \sqrt{\Omega_{r,0}h^2 + \frac{\Omega_{m,0}h^2}{1+z}} - \frac{2\Omega_{r,0}h^2}{\Omega_{m,0}h^2} \left(\sqrt{\Omega_{r,0}h^2 + \frac{\Omega_{m,0}h^2}{1+z}} - \sqrt{\Omega_{r,0}h^2} \right) \right], \quad (4.9)$$

to rewrite ρ_θ as a function of z . In addition, we assume $h = 0.7$ to obtain $\rho_{\theta_5}h^2$. Under these approximations, we get

$$\frac{H_0^{\text{EDE}}}{H_0^{\Lambda\text{CDM}}} \approx 1.05 \quad (4.10)$$

for the $n = 3$ model with $\tilde{g}_4 = 2.95 \times 10^{-6}$ and $M/M_c = 213.1$, which gives $(z_{\max}, \Omega_{\max}) \sim (2500, 0.10)$. Using the value $H_0^{\Lambda\text{CDM}} = 67.4 \text{ km s}^{-1}\text{Mpc}^{-1}$ yields $H_0^{\text{EDE}} = 70.8 \text{ km s}^{-1}\text{Mpc}^{-1}$. If we perform detailed analysis including cosmological perturbations

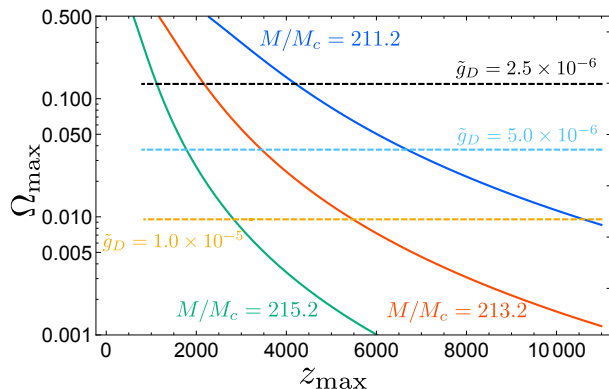


Figure 7: The predicted values of z_{\max} and Ω_{\max} as functions of \tilde{g}_D and M/M_c . The solid vertical lines represent the case with fixed bulk mass and the dashed horizontal lines represent the case with fixed coupling constants. The fixed values are shown next to each line. The three intersections of the cyan dashed line and solid lines correspond to the peaks appeared on the right in Fig. 6, and the three intersections of the red solid line and dashed lines correspond to the peaks appeared on the right in Fig. 5.

without the approximations used so far, we can obtain a more accurate H_0 value and other cosmological parameters, which are required to study the consistency with late time constrains. In addition, we expect that our model can be distinguished from the other solutions to the Hubble tension thorough such analysis, which is left for future studies.

We have analyzed the time evolution of the EDE phase by using the leading effective potential in Eq. (4.1). As a complement to our analysis, we examine subleading corrections to the effective potential and their influence on our discussion. As stated in Sec. 3, the potential (3.6) is obtained in the one-loop approximation. Thus, there are two-loop effects to the leading potential (4.1) as subleading corrections. In addition, to get the leading potential (4.1), we discard $\ell \geq 2$ terms in Eq. (3.6), which also give corrections.

In our scenario, EDE properties for $z > z_{\text{EDE}}$ are mainly determined by the scale of the effective potential for the EDE phase. Thus, higher-order corrections do not give significant effects for $z > z_{\text{EDE}}$. On the other hand, for $z < z_{\text{EDE}}$, the time evolution of the EDE phase is sensitive to the structure of the potential. For example, in the $n = 2$ model, the leading potential is given by $V_{\text{eff}}(\theta_5) \simeq V_{\text{eff}}^{(2)}(\theta_5) \propto \theta_5^4$. If the higher-order corrections include $\mathcal{O}(\theta_5^2)$ terms, the form of the potential near the minimum largely changes. The $\mathcal{O}(\theta_5^2)$ contribution dominates the potential in the region where $|\theta_5|$ is smaller than a critical value θ_c , which is determined by the size of the corrections. Therefore, if θ_c is sufficiently suppressed, we expect that the time evolution of the system is not greatly affected by the corrections.

To estimate the influence of the higher-order corrections on our analysis, let us consider the case where the leading potential $V_{\text{eff}}(\theta_5) \simeq V_{\text{eff}}^{(n)}(\theta_5) \propto \theta_5^{2n}$ receives a correction $\delta V^{(m)} \sim \mathcal{O}(\theta_5^{2m})$ ($n > m \geq 0$). In this case, we can generally parametrize the potential as

$$V_{\text{eff}}(\theta_5) + \delta V^{(m)} \propto \theta_5^{2n} + \epsilon \theta_5^{2m} = \theta_5^{2n} (1 + \epsilon \theta_5^{-2(n-m)}), \quad (4.11)$$

where ϵ gives the size of the correction. For a given ϵ , the correction term grows for $|\theta_5| \lesssim \epsilon^{1/[2(n-m)]} \equiv \theta_C$ in the potential. For a case with $\theta_C \ll 1$, the time evolution of θ_5 is similar to the $\epsilon = 0$ cases, and qualitative results are the same as the discussions given above. We numerically check that the corrections of $\theta_C \lesssim 10^{-2}$ hardly change the results of our numerical analysis.

We can roughly estimate the magnitude of θ_C expected to arise in our model. If a higher-order correction originates from two-loop effects, we expect $|\epsilon| \sim \tilde{g}_D^2/(4\pi^2)$, which is conservatively smaller than 10^{-10} in our numerical calculations with $M_c/M_P = 1.0 \times 10^{-6}$. Thus, we find $\theta_C \sim [\tilde{g}_D^2/(4\pi^2)]^{1/[2(n-m)]} \lesssim 10^{-10/[2(n-m)]}$. To obtain $\theta_C \lesssim 10^{-2}$, the condition $10/[2(n-m)] > 2$ should be satisfied. This condition is naturally satisfied for the $n = 2$ and 3 cases, even for $m = 1$. On the other hand, for $n \geq 4$ cases, our scenario may be disturbed by two-loop corrections to the effective potential. Let us remark that if a smaller value of M_c/M_P is chosen, a required value of \tilde{g}_D^2 also becomes smaller, and higher-order corrections tend to be suppressed. In this case, two-loop corrections in $n \geq 4$ cases are expected to be neglected. For higher-order corrections originating from $\ell \geq 2$ effects, we expect that they are strongly suppressed as $|\epsilon| \sim e^{-M_\varphi/M_c} \sim e^{-100} \sim 10^{-44}$, which cannot impact the results.

Finally, we comment on the effects of non-degenerate bulk masses. The discussion given in this section is based on the case with degenerate bulk mass parameters. If non-degeneracy exists, a bulk mass of a field φ can be expressed by $M + \Delta M_\varphi$, where M is a typical bulk mass scale. For the case with $|\Delta M_\varphi/M| \ll 1$, we can approximately parametrize the effective potential such as in Eq. (4.1) by substituting n_φ for a parameter involving effects of non-zero ΔM_φ . In this case, we can include non-degeneracy into our discussion by changing only the definition of n_φ . Thus, with non-degeneracies, $n \geq 2$ models are possible, while some additional fine-tuning may be required.

5 Discussions and conclusions

The Hubble tension is the discrepancy that should be resolved by some extensions of the standard Λ CDM cosmology. We have shown that the 5D $U(1)_D$ gauge theory, introduced as a dark sector, provides suitable EDE to resolve the tension through the Wilson line phase dynamics. The Wilson line phase associated with the zero-mode of A_5 has a radiatively induced PNCB type potential. A tiny mass scale of the potential, which is suitable to explain EDE, is naturally obtained if the mass parameters in the 5D theory satisfy the relation in Eq. (3.9). In our scenario, M_c , the compactification scale of the extra dimension, is smaller than $\mathcal{O}(10^{-3}M_P)$. We have examined the conditions for the matter contents to give the PNCB type potential that is well approximated by $2n$ -th ($n \geq 2$) polynomial potential around its minima. We have demonstrated numerical calculations of the time evolution of the Wilson line phase in the $n = 2$ and 3 models. The results show that the energy density of the Wilson line phase is a promising candidate for EDE.

More specific models of the 5D gauge theory may have additional implications for both cosmological and particle physics models. Our scenario works in models with S^1 or S^1/\mathbb{Z}_2

compactification. In the latter case, the 4D gauge field associated with $U(1)_D$ acquires a mass of the order of the compactification scale and is decoupled from low-energy physics. On the other hand, for the S^1 case, the zero mode of 4D $U(1)_D$ gauge field remains light and can play some kind of cosmological role as a dark photon. For example, if the dark photon is a massless particle and does not have any interaction with the SM sector, it brings additional relativistic degrees of freedom and a larger value of N_{eff} , which also has been discussed as the solution to the Hubble tension [56, 57]. Alternatively, the dark photon can have a mass and interactions with the SM sector through additional mechanisms, such as Stueckelberg one and a kinetic mixing to the photon. A massive dark photon can be a candidate of dark matter, and the interactions with the SM sector can predict phenomenologically and experimentally interesting features [64]. In addition, we have shown that the $n \geq 2$ models are explained by constrained $U(1)_D$ charges for degenerate bulk matter fields. Such matter contents may be derived from more fundamental particle physics models.

In our scenario, the fundamental parameters in the 5D gauge theory, such as the $U(1)_D$ gauge coupling constant, the bulk mass parameters, and the compactification scale, are related to the property of EDE. Thus, the future progress of cosmological measurements may give constraints and insights into particle physics models based on higher-dimensional gauge theories. To reveal the validity of our scenario, further investigations, such as a complete treatment of the Friedmann equation and analyses of cosmological perturbations, are required. We leave them as future work.

Acknowledgement

The authors are grateful to Carolina Sayuri Takeda for helpful comments on the manuscript. The work of Y.O. is supported in part by the Kyushu University Leading Human Resources Development Fellowship Program.

A Derivation of the solution of Eq. (4.4)

In this appendix, we show that the solution of Eq. (4.4) is given by Eq. (4.5), which ensures that the effective potential for θ_5 satisfies $V_{\text{eff}}(\theta_5) \simeq V_{\text{eff}}^{(n)}(\theta_5)$ around $\theta_5 \simeq 0$ as discussed in Sec. 4. To satisfy Eq. (4.5), $U(1)$ charges and the degrees of freedom of bulk fields are constrained.

Suppose that there are N kinds of bulk matter fields, which are scalars or fermions, with different charges in the 5D $U(1)$ gauge theory as studied in Sec. 4. The effective potential for θ_5 can be written as

$$V_{\text{eff}}(\theta_5) = -V_0 \sum_{i=1}^N d_i (1 - \cos(q_i \theta_5)), \quad (\text{A.1})$$

where d_i and q_i represent the degrees of freedom and a $U(1)$ charge of a field φ_i . We define $|q_i| \neq |q_j|$ for $i \neq j$ and $q_i \neq 0$. Here, we distinguish fields only for absolute values of their $U(1)$ charge. Namely, if multiple fields have the same $U(1)$ charge squared, we denote them by the same label i . The overall constant V_0 is given by Eq. (4.1) and is irrelevant for the following discussion.

The potential (A.1) takes an extreme value for $\theta_5 = 0$ and is expanded around $\theta_5 = 0$ as

$$V_{\text{eff}}(\theta_5) = V_0 \left[\frac{1}{2!} \left(- \sum_{i=1}^N d_i q_i^2 \right) \theta_5^2 + \frac{1}{4!} \left(\sum_{i=1}^N d_i q_i^4 \right) \theta_5^4 + \dots \right]. \quad (\text{A.2})$$

To obtain a potential dominated by the θ_5^{2n} ($n \geq 2$) term for $\theta_5 \simeq 0$, the following $n - 1$ conditions must be satisfied:

$$\sum_{i=1}^N d_i q_i^{2k} = 0, \quad k = 1, \dots, n - 1, \quad (\text{A.3})$$

which can be interpreted as $n - 1$ simultaneous equations for d_i . While there is a trivial solution $d_i = 0$, we don't concern it in the following. If the above condition is satisfied, the effective potential is written as

$$V_{\text{eff}}(\theta_5) = V_0 \frac{(-1)^n}{(2n)!} \left(\sum_{i=1}^N d_i q_i^{2n} \right) \theta_5^{2n} + \mathcal{O}(\theta_5^{2n+2}). \quad (\text{A.4})$$

For a given q_i , we can solve Eq. (A.3) for d_i . To see this, we remark that Eq. (A.3) is not affected by a simultaneous rescaling of d_i as $d_i \rightarrow c d_i$ with an arbitrary parameter c . Thus, the set of parameters $\{d_1, d_2, \dots, d_N\}$ has $N - 1$ degrees of freedom that are relevant to solve Eq. (A.3). Therefore, to obtain a non-trivial solution of the $n - 1$ conditions in Eq. (A.3), the condition $N - 1 \geq n - 1$ should be satisfied.

In the following, we focus on the minimal case with $N = n$. It is convenient to choose the field with $i = n$ as a basis of normalizations of q_i and d_i and define

$$\tilde{Q}_i \equiv \frac{q_i^2}{q_n^2}, \quad \tilde{d}_i \equiv \frac{d_i}{d_n}, \quad (\text{A.5})$$

for $i = 1, \dots, n-1$. Then, the conditions (A.3) can be expressed as

$$1 + \sum_{j=1}^{n-1} \tilde{d}_j \tilde{Q}_j^k = 0, \quad k = 1, \dots, n-1. \quad (\text{A.6})$$

To solve these equations for \tilde{d}_i , let us introduce

$$\begin{aligned} V &= \begin{pmatrix} \tilde{Q}_1 & \tilde{Q}_2 & \cdots & \tilde{Q}_{n-1} \\ \tilde{Q}_1^2 & \tilde{Q}_2^2 & \cdots & \tilde{Q}_{n-1}^2 \\ \vdots & \vdots & \ddots & \vdots \\ \tilde{Q}_1^{n-1} & \tilde{Q}_2^{n-1} & \cdots & \tilde{Q}_{n-1}^{n-1} \end{pmatrix} \\ &= \begin{pmatrix} 1 & 1 & \cdots & 1 \\ \tilde{Q}_1 & \tilde{Q}_2 & \cdots & \tilde{Q}_{n-1} \\ \vdots & \vdots & \ddots & \vdots \\ \tilde{Q}_1^{n-2} & \tilde{Q}_2^{n-2} & \cdots & \tilde{Q}_{n-1}^{n-2} \end{pmatrix} \begin{pmatrix} \tilde{Q}_1 & 0 & \cdots & 0 \\ 0 & \tilde{Q}_2 & \cdots & 0 \\ \vdots & \vdots & \ddots & \vdots \\ 0 & 0 & \cdots & \tilde{Q}_{n-1} \end{pmatrix}, \end{aligned} \quad (\text{A.7})$$

where the first matrix on the right-hand side is known as the Vandermonde matrix. By using V , Eq. (A.6) is rewritten by

$$V \begin{pmatrix} \tilde{d}_1 \\ \vdots \\ \tilde{d}_{n-1} \end{pmatrix} = - \begin{pmatrix} 1 \\ \vdots \\ 1 \end{pmatrix}. \quad (\text{A.8})$$

One sees that the determinant of V is given by

$$\det V = \left(\prod_{\substack{i,j=1 \\ j>i}}^{n-1} (\tilde{Q}_j - \tilde{Q}_i) \right) \left(\prod_{m=1}^{n-1} \tilde{Q}_m \right). \quad (\text{A.9})$$

Since $\tilde{Q}_j \neq \tilde{Q}_i$ for $i \neq j$ and $\tilde{Q}_i \neq 0$ hold in the present case, there exists the inverse of V , denoted by V^{-1} . Therefore, the solution is given by $\tilde{d}_i = -\sum_{k=1}^{n-1} (V^{-1})_{ik}$, where $(V^{-1})_{ik}$ is the (i, k) element of V^{-1} .

To obtain an explicit expression for \tilde{d}_i , let us introduce

$$R_i(\tilde{Q}) = \frac{\tilde{Q}}{\tilde{Q}_i} \prod_{\substack{k=1 \\ k \neq i}}^{n-1} \frac{\tilde{Q} - \tilde{Q}_k}{\tilde{Q}_i - \tilde{Q}_k}. \quad (\text{A.10})$$

By definition, $R_i(\tilde{Q})$ satisfies $R_i(\tilde{Q}_j) = \delta_{ij}$. Here, let us remind that $\sum_{k=1}^{n-1} (V^{-1})_{ik} (V)_{kj} = \sum_{k=1}^{n-1} (V^{-1})_{ik} \tilde{Q}_j^k = \delta_{ij}$ holds, where we have used the fact that the (i, j) element of V is given by $(V)_{ij} = \tilde{Q}_j^i$ as seen from Eq. (A.7). Thus, we find

$$R_i(\tilde{Q}_j) = \sum_{k=1}^{n-1} (V^{-1})_{ik} \tilde{Q}_j^k. \quad (\text{A.11})$$

From the above discussions, \tilde{d}_i is written as follows:

$$\tilde{d}_i = - \sum_{k=1}^{n-1} (V^{-1})_{ik} = -R_i(1) = -\frac{1}{\tilde{Q}_i} \prod_{\substack{k=1 \\ k \neq i}}^{n-1} \frac{1 - \tilde{Q}_k}{\tilde{Q}_i - \tilde{Q}_k}. \quad (\text{A.12})$$

While we have chosen the n -th field as the basis of the normalizations, the above result should not depend on this choice. As expected, one sees that the solution (A.12) is rearranged as

$$\frac{d_i}{d_j} = -\frac{q_j^2}{q_i^2} \prod_{\substack{k=1 \\ k \neq i, j}}^n \frac{q_j^2 - q_k^2}{q_i^2 - q_k^2}, \quad (\text{A.13})$$

which holds for any $i, j \in \{1, \dots, n\}$ and $i \neq j$.

By using the above solution, we can rewrite the leading term of the effective potential in Eq. (A.4). By using \tilde{d}_i and \tilde{Q}_i , the coefficient appearing in Eq. (A.4) is expressed as

$$\frac{(-1)^n}{(2n)!} \sum_{i=1}^n d_i q_i^{2n} = \frac{(-1)^n}{(2n)!} d_n q_n^{2n} \left(1 + \sum_{i=1}^{n-1} \tilde{d}_i \tilde{Q}_i^n \right). \quad (\text{A.14})$$

Substituting Eq. (A.12) into the last factor on the right-hand side of Eq. (A.14), we find

$$\begin{aligned} 1 + \sum_{i=1}^{n-1} \tilde{d}_i \tilde{Q}_i^n &= 1 - \sum_{i=1}^{n-1} \tilde{Q}_i^{n-1} \left[\prod_{\substack{k=1 \\ k \neq i}}^{n-1} \frac{1 - \tilde{Q}_k}{\tilde{Q}_i - \tilde{Q}_k} \right] \\ &= 1 - \tilde{Q}_1^{n-1} \prod_{\substack{k=1 \\ k \neq 1}}^{n-1} \frac{1 - \tilde{Q}_k}{\tilde{Q}_1 - \tilde{Q}_k} \\ &\quad - \tilde{Q}_2^{n-1} \prod_{\substack{k=1 \\ k \neq 2}}^{n-1} \frac{1 - \tilde{Q}_k}{\tilde{Q}_2 - \tilde{Q}_k} \\ &\quad - \dots - \tilde{Q}_{n-1}^{n-1} \prod_{\substack{k=1 \\ k \neq n-1}}^{n-1} \frac{1 - \tilde{Q}_k}{\tilde{Q}_{n-1} - \tilde{Q}_k}. \end{aligned} \quad (\text{A.15})$$

Since the above quantity vanishes for $\tilde{Q}_i = 1$ with an arbitrary i and is linear for any \tilde{Q}_i , we can also write

$$1 + \sum_{i=1}^{n-1} \tilde{d}_i \tilde{Q}_i^n = C(1 - \tilde{Q}_1)(1 - \tilde{Q}_2) \cdots (1 - \tilde{Q}_{n-1}), \quad (\text{A.16})$$

where C is a constant. One sees that $C = 1$ should be satisfied by taking a specific value of \tilde{Q}_i , *e.g.*, $\tilde{Q}_i = 1 - i$. Thus, we get

$$\begin{aligned} \frac{(-1)^n}{(2n)!} \sum_{i=1}^n d_i q_i^{2n} &= \frac{(-1)^n}{(2n)!} d_n q_n^{2n} (1 - \tilde{Q}_1) \cdots (1 - \tilde{Q}_{n-1}) \\ &= \frac{-1}{(2n)!} d_n q_n^2 (q_1^2 - q_n^2) \cdots (q_{n-1}^2 - q_n^2) \\ &= \frac{-1}{(2n)!} d_j q_j^2 \left(\prod_{\substack{k=1 \\ k \neq j}}^n (q_k^2 - q_j^2) \right), \end{aligned} \quad (\text{A.17})$$

where we have used Eq. (A.13) in the last equation. Note that the last expression in Eq. (A.17) holds for any $j \in \{1, \dots, n\}$. Thus, the leading effective potential is written as Eq. (4.6).

References

- [1] N. Aghanim *et al.* [Planck], “Planck 2018 results. VI. Cosmological parameters,” *Astron. Astrophys.* **641**, A6 (2020) [erratum: *Astron. Astrophys.* **652**, C4 (2021)] [[arXiv:1807.06209](#) [astro-ph.CO]].
- [2] A. G. Riess, S. Casertano, W. Yuan, L. M. Macri and D. Scolnic, “Large Magellanic Cloud Cepheid Standards Provide a 1% Foundation for the Determination of the Hubble Constant and Stronger Evidence for Physics beyond Λ CDM,” *Astrophys. J.* **876**, no.1, 85 (2019) [[arXiv:1903.07603](#) [astro-ph.CO]].
- [3] A. G. Riess, W. Yuan, L. M. Macri, D. Scolnic, D. Brout, S. Casertano, D. O. Jones, Y. Murakami, L. Breuval and T. G. Brink, *et al.* “A Comprehensive Measurement of the Local Value of the Hubble Constant with 1 km/s/Mpc Uncertainty from the Hubble Space Telescope and the SH0ES Team,” [[arXiv:2112.04510](#) [astro-ph.CO]].
- [4] E. Di Valentino, O. Mena, S. Pan, L. Visinelli, W. Yang, A. Melchiorri, D. F. Mota, A. G. Riess and J. Silk, “In the realm of the Hubble tension—a review of solutions,” *Class. Quant. Grav.* **38**, no.15, 153001 (2021) [[arXiv:2103.01183](#) [astro-ph.CO]].
- [5] L. A. Anchordoqui, V. Barger, H. Goldberg, X. Huang, D. Marfatia, L. H. M. da Silva and T. J. Weiler, “IceCube neutrinos, decaying dark matter, and the Hubble constant,” *Phys. Rev. D* **92**, no.6, 061301 (2015) [erratum: *Phys. Rev. D* **94**, no.6, 069901 (2016)] [[arXiv:1506.08788](#) [hep-ph]].

- [6] P. Ko, N. Nagata and Y. Tang, “Hidden Charged Dark Matter and Chiral Dark Radiation,” *Phys. Lett. B* **773**, 513-520 (2017) [[arXiv:1706.05605](#) [hep-ph]].
- [7] M. A. Buen-Abad, R. Emami and M. Schmaltz, “Cannibal Dark Matter and Large Scale Structure,” *Phys. Rev. D* **98**, no.8, 083517 (2018) [[arXiv:1803.08062](#) [hep-ph]].
- [8] K. Vattis, S. M. Koushiappas and A. Loeb, “Dark matter decaying in the late Universe can relieve the H_0 tension,” *Phys. Rev. D* **99**, no.12, 121302 (2019) [[arXiv:1903.06220](#) [astro-ph.CO]].
- [9] K. L. Pandey, T. Karwal and S. Das, “Alleviating the H_0 and σ_8 anomalies with a decaying dark matter model,” *JCAP* **07**, 026 (2020) [[arXiv:1902.10636](#) [astro-ph.CO]].
- [10] A. Hryczuk and K. Jodłowski, “Self-interacting dark matter from late decays and the H_0 tension,” *Phys. Rev. D* **102**, no.4, 043024 (2020) [[arXiv:2006.16139](#) [hep-ph]].
- [11] S. Kumar and R. C. Nunes, “Probing the interaction between dark matter and dark energy in the presence of massive neutrinos,” *Phys. Rev. D* **94**, no.12, 123511 (2016) [[arXiv:1608.02454](#) [astro-ph.CO]].
- [12] E. Di Valentino, A. Melchiorri and O. Mena, “Can interacting dark energy solve the H_0 tension?,” *Phys. Rev. D* **96**, no.4, 043503 (2017) [[arXiv:1704.08342](#) [astro-ph.CO]].
- [13] A. Banihashemi, N. Khosravi and A. H. Shirazi, “Ginzburg-Landau Theory of Dark Energy: A Framework to Study Both Temporal and Spatial Cosmological Tensions Simultaneously,” *Phys. Rev. D* **99**, no.8, 083509 (2019) [[arXiv:1810.11007](#) [astro-ph.CO]]; “Phase transition in the dark sector as a proposal to lessen cosmological tensions,” *Phys. Rev. D* **101**, no.12, 123521 (2020) [[arXiv:1808.02472](#) [astro-ph.CO]].
- [14] J. Renk, M. Zumalacárregui, F. Montanari and A. Barreira, “Galileon gravity in light of ISW, CMB, BAO and H_0 data,” *JCAP* **10**, 020 (2017) [[arXiv:1707.02263](#) [astro-ph.CO]].
- [15] N. Khosravi, S. Baghran, N. Afshordi and N. Altamirano, “ H_0 tension as a hint for a transition in gravitational theory,” *Phys. Rev. D* **99**, no.10, 103526 (2019) [[arXiv:1710.09366](#) [astro-ph.CO]].
- [16] S. F. Yan, P. Zhang, J. W. Chen, X. Z. Zhang, Y. F. Cai and E. N. Saridakis, “Interpreting cosmological tensions from the effective field theory of torsional gravity,” *Phys. Rev. D* **101**, no.12, 121301 (2020) [[arXiv:1909.06388](#) [astro-ph.CO]].
- [17] S. D. Odintsov, D. Sáez-Chillón Gómez and G. S. Sharov, “Analyzing the H_0 tension in $F(R)$ gravity models,” *Nucl. Phys. B* **966**, 115377 (2021) [[arXiv:2011.03957](#) [gr-qc]].
- [18] M. G. Dainotti, B. De Simone, T. Schiavone, G. Montani, E. Rinaldi, G. Lambiase, M. Bogdan and S. Ugale, “On the Evolution of the Hubble Constant with the SNe Ia Pantheon Sample and Baryon Acoustic Oscillations: A Feasibility Study for GRB-Cosmology in 2030,” *Galaxies* **10**, no.1, 24 (2022) [[arXiv:2201.09848](#) [astro-ph.CO]].

- [19] S. Vagnozzi, “New physics in light of the H_0 tension: An alternative view,” Phys. Rev. D **102**, no.2, 023518 (2020) [[arXiv:1907.07569](#) [astro-ph.CO]].
- [20] G. Alestas, L. Kazantzidis and L. Perivolaropoulos, “ H_0 tension, phantom dark energy, and cosmological parameter degeneracies,” Phys. Rev. D **101**, no.12, 123516 (2020) [[arXiv:2004.08363](#) [astro-ph.CO]].
- [21] E. Di Valentino, A. Melchiorri and J. Silk, “Reconciling Planck with the local value of H_0 in extended parameter space,” Phys. Lett. B **761**, 242-246 (2016) [[arXiv:1606.00634](#) [astro-ph.CO]].
- [22] E. Di Valentino, A. Melchiorri, E. V. Linder and J. Silk, “Constraining Dark Energy Dynamics in Extended Parameter Space,” Phys. Rev. D **96**, no.2, 023523 (2017) [[arXiv:1704.00762](#) [astro-ph.CO]].
- [23] S. Vagnozzi, S. Dhawan, M. Gerbino, K. Freese, A. Goobar and O. Mena, “Constraints on the sum of the neutrino masses in dynamical dark energy models with $w(z) \geq -1$ are tighter than those obtained in Λ CDM,” Phys. Rev. D **98**, no.8, 083501 (2018) [[arXiv:1801.08553](#) [astro-ph.CO]].
- [24] W. Yang, S. Pan, E. Di Valentino, E. N. Saridakis and S. Chakraborty, “Observational constraints on one-parameter dynamical dark-energy parametrizations and the H_0 tension,” Phys. Rev. D **99**, no.4, 043543 (2019) [[arXiv:1810.05141](#) [astro-ph.CO]].
- [25] E. Di Valentino, A. Melchiorri, O. Mena and S. Vagnozzi, “Nonminimal dark sector physics and cosmological tensions,” Phys. Rev. D **101**, no.6, 063502 (2020) [[arXiv:1910.09853](#) [astro-ph.CO]].
- [26] E. Di Valentino, A. Mukherjee and A. A. Sen, “Dark Energy with Phantom Crossing and the H_0 Tension,” Entropy **23**, no.4, 404 (2021) [[arXiv:2005.12587](#) [astro-ph.CO]].
- [27] M. G. Dainotti, B. De Simone, T. Schiavone, G. Montani, E. Rinaldi and G. Lambiase, “On the Hubble constant tension in the SNe Ia Pantheon sample,” Astrophys. J. **912**, no.2, 150 (2021) [[arXiv:2103.02117](#) [astro-ph.CO]].
- [28] T. Karwal and M. Kamionkowski, “Dark energy at early times, the Hubble parameter, and the string axiverse,” Phys. Rev. D **94**, no.10, 103523 (2016) [[arXiv:1608.01309](#) [astro-ph.CO]].
- [29] E. Mörtzell and S. Dhawan, “Does the Hubble constant tension call for new physics?,” JCAP **09**, 025 (2018) [[arXiv:1801.07260](#) [astro-ph.CO]].
- [30] V. Poulin, T. L. Smith, T. Karwal and M. Kamionkowski, “Early Dark Energy Can Resolve The Hubble Tension,” Phys. Rev. Lett. **122**, no.22, 221301 (2019) [[arXiv:1811.04083](#) [astro-ph.CO]].
- [31] T. L. Smith, V. Poulin and M. A. Amin, “Oscillating scalar fields and the Hubble tension: a resolution with novel signatures,” Phys. Rev. D **101**, no.6, 063523 (2020) [[arXiv:1908.06995](#) [astro-ph.CO]].

- [32] J. C. Hill, E. McDonough, M. W. Toomey and S. Alexander, “Early dark energy does not restore cosmological concordance,” *Phys. Rev. D* **102**, no.4, 043507 (2020) [[arXiv:2003.07355](#) [astro-ph.CO]].
- [33] M. Kamionkowski, J. Pradler and D. G. E. Walker, “Dark energy from the string axiverse,” *Phys. Rev. Lett.* **113**, no.25, 251302 (2014) [[arXiv:1409.0549](#) [hep-ph]].
- [34] V. Poulin, T. L. Smith, D. Grin, T. Karwal and M. Kamionkowski, “Cosmological implications of ultralight axionlike fields,” *Phys. Rev. D* **98**, no.8, 083525 (2018) [[arXiv:1806.10608](#) [astro-ph.CO]].
- [35] P. Agrawal, F. Y. Cyr-Racine, D. Pinner and L. Randall, “Rock ‘n’ Roll Solutions to the Hubble Tension,” [[arXiv:1904.01016](#) [astro-ph.CO]].
- [36] S. Alexander and E. McDonough, “Axion-Dilaton Destabilization and the Hubble Tension,” *Phys. Lett. B* **797**, 134830 (2019) [[arXiv:1904.08912](#) [astro-ph.CO]].
- [37] F. Niedermann and M. S. Sloth, “New early dark energy,” *Phys. Rev. D* **103**, no.4, L041303 (2021) [[arXiv:1910.10739](#) [astro-ph.CO]].
- [38] K. V. Berghaus and T. Karwal, “Thermal Friction as a Solution to the Hubble Tension,” *Phys. Rev. D* **101**, no.8, 083537 (2020) [[arXiv:1911.06281](#) [astro-ph.CO]].
- [39] J. Sakstein and M. Trodden, “Early Dark Energy from Massive Neutrinos as a Natural Resolution of the Hubble Tension,” *Phys. Rev. Lett.* **124**, no.16, 161301 (2020) [[arXiv:1911.11760](#) [astro-ph.CO]].
- [40] G. Ye and Y. S. Piao, “Is the Hubble tension a hint of AdS phase around recombination?,” *Phys. Rev. D* **101**, no.8, 083507 (2020) [[arXiv:2001.02451](#) [astro-ph.CO]].
- [41] A. Chudaykin, D. Gorbunov and N. Nedelko, “Combined analysis of Planck and SPTPol data favors the early dark energy models,” *JCAP* **08**, 013 (2020) [[arXiv:2004.13046](#) [astro-ph.CO]].
- [42] B. S. Haridasu, M. Viel and N. Vittorio, “Sources of H_0 -tension in dark energy scenarios,” *Phys. Rev. D* **103**, no.6, 063539 (2021) [[arXiv:2012.10324](#) [astro-ph.CO]].
- [43] S. Vagnozzi, “Consistency tests of Λ CDM from the early integrated Sachs-Wolfe effect: Implications for early-time new physics and the Hubble tension,” *Phys. Rev. D* **104**, no.6, 063524 (2021) [[arXiv:2105.10425](#) [astro-ph.CO]].
- [44] K. V. Berghaus and T. Karwal, “Thermal Friction as a Solution to the Hubble and Large-Scale Structure Tensions,” [[arXiv:2204.09133](#) [astro-ph.CO]].
- [45] For a review, see *e.g.*, A. D. Linde, “Inflationary Cosmology,” *Lect. Notes Phys.* **738**, 1-54 (2008) [[arXiv:0705.0164](#) [hep-th]].
- [46] For a review, see *e.g.*, S. Tsujikawa,, “Quintessence: A Review,” *Class. Quant. Grav.* **30**, 214003 (2013) [[arXiv:1304.1961](#) [gr-qc]].

- [47] M. S. Turner, “Coherent Scalar Field Oscillations in an Expanding Universe,” *Phys. Rev. D* **28**, 1243 (1983).
- [48] N. Arkani-Hamed, H. C. Cheng, P. Creminelli and L. Randall, “Extra natural inflation,” *Phys. Rev. Lett.* **90**, 221302 (2003) [[arXiv:hep-th/0301218](#) [hep-th]]; “Pseudonatural inflation,” *JCAP* **07**, 003 (2003) [[arXiv:hep-th/0302034](#) [hep-th]].
- [49] L. Pilo, D. A. J. Rayner and A. Riotto, “Gauge quintessence,” *Phys. Rev. D* **68**, 043503 (2003) [[arXiv:hep-ph/0302087](#) [hep-ph]].
- [50] J. C. Mather, D. J. Fixsen, R. A. Shafer, C. Mosier and D. T. Wilkinson, “Calibrator design for the COBE far infrared absolute spectrophotometer (FIRAS),” *Astrophys. J.* **512**, 511-520 (1999) [[arXiv:astro-ph/9810373](#) [astro-ph]].
- [51] J. Lesgourgues and S. Pastor, “Massive neutrinos and cosmology,” *Phys. Rept.* **429**, 307-379 (2006) [[arXiv:astro-ph/0603494](#) [astro-ph]].
- [52] K. Akita and M. Yamaguchi, “A precision calculation of relic neutrino decoupling,” *JCAP* **08**, 012 (2020) [[arXiv:2005.07047](#) [hep-ph]].
- [53] S. Dimopoulos, S. Kachru, J. McGreevy and J. G. Wacker, “N-flation,” *JCAP* **08**, 003 (2008) [[arXiv:hep-th/0507205](#) [hep-th]].
- [54] D. J. E. Marsh, “Axion Cosmology,” *Phys. Rept.* **643**, 1-79 (2016) [[arXiv:1510.07633](#) [astro-ph.CO]].
- [55] A. G. Riess, L. M. Macri, S. L. Hoffmann, D. Scolnic, S. Casertano, A. V. Filippenko, B. E. Tucker, M. J. Reid, D. O. Jones and J. M. Silverman, *et al.* “A 2.4% Determination of the Local Value of the Hubble Constant,” *Astrophys. J.* **826**, no.1, 56 (2016) [[arXiv:1604.01424](#) [astro-ph.CO]].
- [56] F. D’Eramo, R. Z. Ferreira, A. Notari and J. L. Bernal, “Hot Axions and the H_0 tension,” *JCAP* **11**, 014 (2018) [[arXiv:1808.07430](#) [hep-ph]].
- [57] C. D. Kreisch, F. Y. Cyr-Racine and O. Doré, “Neutrino puzzle: Anomalies, interactions, and cosmological tensions,” *Phys. Rev. D* **101**, no.12, 123505 (2020) [[arXiv:1902.00534](#) [astro-ph.CO]].
- [58] A. Hebecker and J. March-Russell, “The structure of GUT breaking by orbifolding,” *Nucl. Phys. B* **625**, 128-150 (2002) [[arXiv:hep-ph/0107039](#) [hep-ph]].
- [59] N. Haba, Y. Kawamura and K. Oda, “Dynamical Rearrangement of Theta Parameter in Presence of Mixed Chern-Simons Term,” *Phys. Rev. D* **78**, 085021 (2008) [[arXiv:0803.4380](#) [hep-ph]].
- [60] Y. Kawamura and T. Miura, “ μ Parameter from Dynamical Rearrangement of U(1) and θ Parameter,” *Int. J. Mod. Phys. A* **27**, 1250023 (2012) [[arXiv:1108.1004](#) [hep-ph]].

- [61] Y. Abe, Y. Goto, Y. Kawamura and Y. Nishikawa, “Conjugate boundary condition, hidden particles, and gauge-Higgs inflation,” *Mod. Phys. Lett. A* **31**, no.35, 1650208 (2016) [[arXiv:1608.06393](#) [hep-ph]].
- [62] A. Delgado, A. Pomarol and M. Quiros, “Supersymmetry and electroweak breaking from extra dimensions at the TeV scale,” *Phys. Rev. D* **60**, 095008 (1999) [[arXiv:hep-ph/9812489](#) [hep-ph]].
- [63] N. Maru and K. Takenaga, “Effects of bulk mass in gauge-Higgs unification,” *Phys. Lett. B* **637**, 287-294 (2006) [[arXiv:hep-ph/0602149](#) [hep-ph]].
- [64] M. Fabbrichesi, E. Gabrielli and G. Lanfranchi, “The Dark Photon,” [[arXiv:2005.01515](#) [hep-ph]].